# Incremental variational homogenization of elastoplastic composites with isotropic and Armstrong-Frederick type nonlinear kinematic hardening

Antoine Lucchetta, François Auslender, Michel Bornert, Djimédo Kondo

# Incremental variational homogenization of elastoplastic composites with isotropic and Armstrong-Frederick type nonlinear kinematic hardening

Antoine Lucchetta[a], François Auslender[b,*], Michel Bornert[c], Djimédo Kondo[a]

[a]*Sorbonne Université, Institut Jean le Rond ∂'Alembert, UMR 7190 CNRS, 4, Place Jussieu, 75252 Paris Cedex 05, France*
[b]*Université Clermont Auvergne, Institut Pascal (UCA/SIGMA/CNRS UMR 6602), BP 10448, 63000 Clermont-Ferrand, France*
[c]*Laboratoire Navier, Université Gustave Eiffel, ENPC, UMR 8205 CNRS, 77455 Marne-la-Vallée Cedex, France*

**Abstract**

In order to investigate the behavior of elastoplastic composites exhibiting both isotropic and *nonlinear* kinematic hardening, we extend the Double Incremental Variational (DIV) formulation of Lucchetta et al. [1], based on both the incremental variational principles introduced by Lahellec and Suquet [2] and the formulation proposed by Agoras et al. [3]. However, the Armstrong-Frederick model [4], which is very often used to describe nonlinear kinematic hardening and refers to the framework of non-associated plasticity [5], cannot be handled within the framework of generalized standard materials as required by the incremental variational principles on which the DIV formulation relies. That is why we work with an approximation of this model, namely the modified Chaboche model [6]. As the dissipation potential associated with this model depends on internal variables,

☆Corresponding author
*François Auslender; Tel.: 00 33 (0)4 73 28 81 24; Fax: 00 33 (0)4 73 28 80 27; Email: francois.auslender@uca.fr

we have to extend the incremental variational principles of Lahellec and Suquet to such a situation. Then, we apply twice the variational procedure of Ponte Castañeda [7], first to linearize the local behavior and then to deal with the intraphase heterogeneity of the thermoelastic Linear Comparison Composite (LCC) induced by the linearisation step. The resulting thermoelastic LCC with per-phase homogeneous properties is homogenized by classical linear schemes. We develop and implement this new incremental variational procedure for two-phase matrix-inclusions composites with an isotropic elastoplastic matrix exhibiting combined isotropic and nonlinear kinematic hardening. For various cyclic loadings, the predictions of the proposed DIV formulation compare favorably with Finite Element simulations based on the Armstrong-Frederick model.
*Keywords:* Elastoplastic composites, Nonlinear kinematic hardening, Isotropic hardening, Homogenization, Variational methods, cyclic loadings

## 1. Introduction

The aim of this paper is to extend to nonlinear kinematic hardening the mean field homogenization formulation recently proposed by Lucchetta et al. [1] to predict the behavior of composite materials made of elastoplastic phases which exhibit linear kinematic and isotropic hardening. This formulation relies on incremental variational principles initially proposed by Lahellec and Suquet [2] to predict the effective behavior of composites made of Generalized Standard Materials (GSM, Halphen and Nguyen [8]), when dissipative and conservative effects are strongly coupled. It was restricted to linear kinematic hardening. However, it is well known that such a constitutive relation is not sufficient to describe the experimentally observed behavior of many elastoplastic materials, especially when they

are submitted to cyclic loading conditions (Lemaitre and Chaboche [9]). For such materials, more elaborated constitutive relations have been proposed, such as the Armstrong and Frederick (AF) model [4] which introduced nonlinear kinematic hardening. As recalled later in this paper, this model however is non-associated, and therefore cannot be handled in the framework of GSM. As such, it cannot be directly implemented in the above mentioned incremental variational principles. In order to homogenize elastoplastic composites made of phases exhibiting this kind of nonlinear kinematic hardening within the framework of the above mentioned incremental variational principles, a slightly modified formulation, the modified Chaboche model [6], is considered here. This model, the expressions of which are briefly recalled in Section 3, derives from two potentials, namely the free energy $w(\boldsymbol{\varepsilon}, \boldsymbol{\alpha})$ and the dissipation potential $\varphi(\dot{\boldsymbol{\alpha}}, \boldsymbol{\alpha})$ where $\boldsymbol{\varepsilon}$ is the infinitesimal local strain and $\boldsymbol{\alpha}$ is a set of internal variables. It should be noted that the dissipation potential of the modified Chaboche model not only depends on the rate of internal variables but also evolves with the internal variables (i.e. $\varphi \equiv \varphi(\dot{\boldsymbol{\alpha}}, \boldsymbol{\alpha})$), which play the role of a state parameter in agreement with Nguyen [10] and Germain et al. [11]. Due to this additional dependance of $\varphi$, the earlier variational formulation has to be slightly modified as described in Section 2. A main purpose of this paper is to provide (Section 4) the details of the derivation of the DIV approach in the case of composites which phases exhibit Armstrong-Frederick nonlinear kinematic hardening. Note that the here derived DIV model is related to the particular form of the chosen nonlinear kinematic hardening law, that is the Armstrong-Frederick rule. New specific derivations would be required for another nonlinear kinematic rule but could be based on a similar methodology. Namely, to derive the presented DIV approach, we make use of the key idea

proposed by Agoras et al. [3], which consists in addressing sequentially, first the linearization of the local behavior and then the uniformization of the resulting LCC which exhibits a heterogeneous polarization inside the phases. This is however done within a total form of the incremental variational procedure in the line of Lahellec and Suquet [2] and not an incremental one as adopted by Agoras et al. [3]. The DIV procedure is then applied to reinforced isotropic elastoplastic composites with both isotropic and nonlinear kinematic hardening, submitted to cyclic loading conditions (Section 5).

The homogenization of materials made of elastoplastic constituents has been the subject of many publications in recent years among which several are in the line of the pioneering work of Lahellec and Suquet [2]. An alternative incremental variational procedure has been proposed by Ortiz and Stainier [12] and applied to composites with isotropic hardening by Brassart et al. [13]. Linear kinematic hardening has explicitly been considered in the papers of Lahellec and Suquet [14], Boudet et al. [15] and Lucchetta et al. [1], and was in some cases combined with isotropic hardening. For more details regarding the homogenization of elastoplastic composites, the interested reader may refer to the bibliography in the above papers, and in particular to the work of Agoras et al. [3] who proposed a specific extension but who did not consider hardening. It is also worth noting the recent work of Idiart and Lahellec [16] who introduced comparison solids with pointwise heterogeneous properties which lead to a better prediction of the effective stress for elastoviscoplastic composites submitted to a rotating deformation loading history. More recently, Mercier et al. [17] have applied the so-called tangent formulation (Molinari et al. [18]), extended to elasto-viscoplastic composites (Mercier and Molinari [19]), to the particular case of combined linear kinematic

and isotropic hardening.

Very few works however address the situation under consideration here, namely of nonlinear kinematic hardening. One of these (Doghri and Ouaar [20]) relies on the classical incremental formulation of Hill [21], not based on a variational formulation and not accounting for intraphase field fluctuations. On another hand, Michel and Suquet [22] address this situation with the so-called NTFA methodology which makes use of a set of complex local fields, called plastic modes, which need to be computed numerically for a specific virtual microstructure.

## 2. Incremental variational principle for the effective behavior of inelastic composites

We present here a slightly modified version of the local and effective variational principles, initially introduced by Lahellec and Suquet [2], on which the nonlinear homogenization DIV procedure described in Section 4 relies.

### *2.1. Generalized standard materials*

The composite materials considered in this study are comprised of phases for which the constitutive laws derive from two thermodynamic potentials. The free-energy $w(\boldsymbol{\varepsilon}, \boldsymbol{\alpha})$ depends on both the infinitesimal strain $\boldsymbol{\varepsilon}$ and a finite set of internal variables $\boldsymbol{\alpha}$. The Cauchy stress $\boldsymbol{\sigma}$ and the irreversible driving forces $\boldsymbol{\mathcal{A}}_\alpha$ are derived from this potential through the state laws as

$$\boldsymbol{\sigma} = \frac{\partial w}{\partial \boldsymbol{\varepsilon}}(\boldsymbol{\varepsilon}, \boldsymbol{\alpha}) \ , \quad \boldsymbol{\mathcal{A}}_\alpha = -\frac{\partial w}{\partial \boldsymbol{\alpha}}(\boldsymbol{\varepsilon}, \boldsymbol{\alpha}). \tag{1}$$

The evolution of the internal variables $\boldsymbol{\alpha}$ is derived from the dissipation potential $\varphi(\dot{\boldsymbol{\alpha}}, \boldsymbol{\alpha})$ through

$$\boldsymbol{\mathcal{A}}_\alpha = \frac{\partial \varphi}{\partial \dot{\boldsymbol{\alpha}}}(\dot{\boldsymbol{\alpha}}, \boldsymbol{\alpha}) \ , \quad \text{or equivalently} \quad \dot{\boldsymbol{\alpha}} = \frac{\partial \varphi^*}{\partial \boldsymbol{\mathcal{A}}_\alpha}(\boldsymbol{\mathcal{A}}_\alpha, \boldsymbol{\alpha}). \tag{2}$$

The dual potential $\varphi^*$ is the Legendre-Fenchel transform of $\varphi$ with respect to (w.r.t.) $\dot{\boldsymbol{\alpha}}$ defined by[1] $\varphi^*(\boldsymbol{\mathcal{A}}_\alpha, \boldsymbol{\alpha}) = \sup_{\dot{\alpha}} \left[\boldsymbol{\mathcal{A}}_\alpha \dot{\boldsymbol{\alpha}} - \varphi(\dot{\boldsymbol{\alpha}}, \boldsymbol{\alpha})\right]$ while $\boldsymbol{\alpha}$ plays the role of a parameter representing the thermodynamical state for both dissipation potentials $\varphi$ and $\varphi^*$. If $w$ and $\varphi$ are convex functions of their arguments $\dot{\boldsymbol{\alpha}}$ and $\boldsymbol{\mathcal{A}}_\alpha$, and minimal at $\dot{\boldsymbol{\alpha}} = \mathbf{0}$ and $\boldsymbol{\mathcal{A}}_\alpha = \mathbf{0}$, Eqs. (1) and (2) define the constitutive laws of a generalized standard material (GSM) in the sense of Germain et al. [11] and Nguyen [10]. They can be rewritten as the following system of two coupled equations

$$\boldsymbol{\sigma} = \frac{\partial w}{\partial \boldsymbol{\varepsilon}}(\boldsymbol{\varepsilon}, \boldsymbol{\alpha}) \ , \quad \frac{\partial w}{\partial \boldsymbol{\alpha}}(\boldsymbol{\varepsilon}, \boldsymbol{\alpha}) + \frac{\partial \varphi}{\partial \dot{\boldsymbol{\alpha}}}(\dot{\boldsymbol{\alpha}}, \boldsymbol{\alpha}) = 0. \tag{3}$$

Again, it should be noted that unlike the GSM introduced by Nguyen and Halphen [8], the dissipation potential $\varphi$ considered in the present work depends on both the rates of the state variables $\dot{\boldsymbol{\alpha}}$ and on the state variables $\boldsymbol{\alpha}$ themselves as suggested in Germain et al.[11] and in Nguyen [10] (see also [23]). For this reason, a rewriting of the incremental variational principles introduced by Lahellec and Suquet [2], which relies on "classical" GSM for which the dissipation potential only depends on $\dot{\boldsymbol{\alpha}}$, is required and presented in the following section.

[1] For non differentiable dissipation potentials, the constitutive relations (2) should be replaced by $\boldsymbol{\mathcal{A}}_\alpha \in \partial_{\dot{\boldsymbol{\alpha}}} \varphi(\dot{\boldsymbol{\alpha}}, \boldsymbol{\alpha})$ or $\dot{\boldsymbol{\alpha}} \in \partial_{\boldsymbol{\mathcal{A}}_\alpha} \varphi^*(\boldsymbol{\mathcal{A}}_\alpha, \boldsymbol{\alpha})$, where $\partial_{\dot{\boldsymbol{\alpha}}} \varphi(\dot{\boldsymbol{\alpha}}, \boldsymbol{\alpha})$ and $\partial_{\boldsymbol{\mathcal{A}}_\alpha} \varphi^*(\boldsymbol{\mathcal{A}}_\alpha, \boldsymbol{\alpha})$ denote the subdifferentials of the dissipative functions $\varphi(\dot{\boldsymbol{\alpha}}, \boldsymbol{\alpha})$ and $\varphi^*(\boldsymbol{\mathcal{A}}_\alpha, \boldsymbol{\alpha})$ w.r.t. $\dot{\boldsymbol{\alpha}}$ and $\boldsymbol{\mathcal{A}}_\alpha$, respectively.

*2.2. Incremental potential*

Following Lahellec and Suquet [2], we make use of a "total" formulation, i.e., depending on $\boldsymbol{\varepsilon}$ and $\boldsymbol{\alpha}$, instead of a rate one, that would depend on $\dot{\boldsymbol{\varepsilon}}$ and $\dot{\boldsymbol{\alpha}}$ as in Lahellec and Suquet [14].

The time interval $[0, T]$ of the loading history applied to the composite material under consideration is discretized into $M$ time steps, not necessarily of identical duration and characterized by the set $\{t_0 = 0, t_1, ..., t_n, t_{n+1}, ..., t_M = T\}$. For convenience, the value $f(t_n)$ of a function $f$ at time $t_n$ and the time step $t_{n+1} - t_n$ are denoted $f_n$ and $\Delta t$, respectively. Furthermore, for ease of notation, we will omit in the sequel the index $n + 1$ for the variables computed at time $t_{n+1}$ (i.e. $\boldsymbol{\varepsilon} \equiv \boldsymbol{\varepsilon}_{n+1}$). The time discretization of Eq. (3) according to an Euler implicit scheme results in the following equations

$$\boldsymbol{\sigma} = \frac{\partial w}{\partial \boldsymbol{\varepsilon}}(\boldsymbol{\varepsilon}, \boldsymbol{\alpha}), \qquad \frac{\partial w}{\partial \boldsymbol{\alpha}}(\boldsymbol{\varepsilon}, \boldsymbol{\alpha}) + \frac{\partial \varphi}{\partial \dot{\boldsymbol{\alpha}}}\left(\frac{\boldsymbol{\alpha} - \boldsymbol{\alpha}_n}{\Delta t}, \boldsymbol{\alpha}\right) = 0. \tag{4}$$

where the internal variables $\boldsymbol{\alpha}_n$ are assumed to be known from the former step. Inspired by Lahellec and Suquet [2], we introduce the following variational problem

$$w_\Delta(\boldsymbol{\varepsilon}, \boldsymbol{\alpha}_n) = \inf_{\boldsymbol{\alpha}} J(\boldsymbol{\varepsilon}, \boldsymbol{\alpha}, \boldsymbol{\alpha}_n), \tag{5}$$

with

$$J(\boldsymbol{\varepsilon}, \boldsymbol{\alpha}, \boldsymbol{\alpha}_n) = w(\boldsymbol{\varepsilon}, \boldsymbol{\alpha}) + \Delta t\, \varphi\left(\frac{\boldsymbol{\alpha} - \boldsymbol{\alpha}_n}{\Delta t}, \boldsymbol{\alpha}_n\right). \tag{6}$$

Its Euler-Lagrange equations are given by

$$\frac{\partial w}{\partial \boldsymbol{\alpha}}(\boldsymbol{\varepsilon}, \boldsymbol{\alpha}) + \frac{\partial \varphi}{\partial \dot{\boldsymbol{\alpha}}}\left(\frac{\boldsymbol{\alpha} - \boldsymbol{\alpha}_n}{\Delta t}, \boldsymbol{\alpha}_n\right) = 0. \tag{7}$$

In the sequel, we consider a regular dissipation function $\varphi$ (see expressions (23) and (24)) such that $\frac{\partial \varphi}{\partial \dot{\boldsymbol{\alpha}}}(\dot{\boldsymbol{\alpha}}, \boldsymbol{\alpha})$ is $\mathcal{C}^1$ with respect to $\boldsymbol{\alpha}$, thus implying that $\frac{\partial \varphi}{\partial \dot{\boldsymbol{\alpha}}}(\dot{\boldsymbol{\alpha}}, \boldsymbol{\alpha}) \simeq \frac{\partial \varphi}{\partial \dot{\boldsymbol{\alpha}}}(\dot{\boldsymbol{\alpha}}, \boldsymbol{\alpha}_n)$ for $\boldsymbol{\alpha}$ close enough to $\boldsymbol{\alpha}_n$. Accordingly, given slow variations in time of internal variables, Eq. $(4)_2$ is equivalent to Eq. (7) and thus corresponds to the Euler Lagrange equations of the variational problem (5).

Due to the stationarity of $J$ w.r.t. $\boldsymbol{\alpha}$, the stress tensor defined by Eq. $(4)_1$ reads

$$\boldsymbol{\sigma} = \frac{\partial\, w_\Delta}{\partial\, \boldsymbol{\varepsilon}}(\boldsymbol{\varepsilon}, \boldsymbol{\alpha}_n). \tag{8}$$

As in Lahellec and Suquet [2], $J$ and $w_\Delta$ are referred in the sequel as the incremental potential and the condensed incremental potential.

Note that alternative more sophisticated implicit discretizations could have been proposed in the definition of the incremental variational principle given by Eqs. (5) and (6). For instance, similarly to the work of Brassart and Stainier [24], the variational principle (5) might be modified by making use in Eq. (6) of a mid-point rule, i.e. $\theta\boldsymbol{\alpha} + (1-\theta)\boldsymbol{\alpha}_n$, to approximate the internal variable $\boldsymbol{\alpha}$ in the dissipation potential instead of the explicit discretisation $\boldsymbol{\alpha}_n$ considered in our approach. This implicit discretization might be interesting since it would potentially lead to a more robust algorithm able to use larger time steps $\Delta t$ than the ones used here. However, such a modified version of the incremental variational principle induces a supplementary term $\Delta t\theta \frac{\partial \varphi}{\partial \boldsymbol{\alpha}}$ in its Euler-Lagrange equations. This new term is not easy to evaluate in a mean-field framework and its derivation would significantly complexify the DIV model.

*2.3. Inelastic composites: effective incremental potential*

We consider composite materials made of $N$ different homogeneous constituents occupying domains $\Omega^{(r)}$ with characteristic functions $\chi^{(r)}$ and volume fractions $c^{(r)}$. The phases are assumed to be randomly distributed in a representative volume element (RVE) occupying a volume $\Omega = \cup_{r=1}^{N} \Omega^{(r)}$. The constitutive behavior of each phase $r$ is governed by two potentials $w^{(r)}$ and $\varphi^{(r)}$ in the framework of the GSM such that the local fields $\boldsymbol{\sigma}(\underline{x}, t)$, $\boldsymbol{\varepsilon}(\underline{x}, t)$ and $\boldsymbol{\alpha}(\underline{x}, t)$ at each position $\underline{x}$ satisfy Eq. (3) for the free-energy function $w$ and the dissipation potential $\varphi$ defined by

$$w(\underline{x}, \boldsymbol{\varepsilon}, \boldsymbol{\alpha}) = \sum_{r=1}^{N} w^{(r)}(\boldsymbol{\varepsilon}, \boldsymbol{\alpha})\, \chi^{(r)}(\underline{x}) \quad \text{and} \quad \varphi(\underline{x}, \dot{\boldsymbol{\alpha}}, \boldsymbol{\alpha}) = \sum_{r=1}^{N} \varphi^{(r)}(\dot{\boldsymbol{\alpha}}, \boldsymbol{\alpha})\, \chi^{(r)}(\underline{x}). \tag{9}$$

In the following, we will consider the first and second-order moments as well as the fluctuations of the local fields. The notation $< \, . \, >$ represents the volume average over the composite $\Omega$. The compact notation $\bar{\boldsymbol{a}}^{(r)} =< \boldsymbol{a} >^{(r)}$, where $< \, . \, >^{(r)}$ stands for the volume average over the phase $\Omega^{(r)}$, will also be used to denote the first-order moment of any field $\boldsymbol{a}(\underline{x})$ over the phase $r$. The notation $\overline{\overline{a}}^{(r)} = \sqrt{\iota \langle \boldsymbol{a}_d : \boldsymbol{a}_d \rangle^{(r)}}$ represents the second-order moment of a second-order tensor field $\boldsymbol{a}$ with $\iota = \frac{2}{3}$ for a strain field and $\iota = \frac{3}{2}$ for a stress field and $\boldsymbol{a}_d$ denotes the deviatoric part of the tensor $\boldsymbol{a}$. Finally, the fluctuations of a second-order tensor field $\boldsymbol{a}$ will be quantified by its fourth-order covariance tensor:

$$C^{(r)}(\boldsymbol{a}) = \left\langle \left(\boldsymbol{a} - \overline{\boldsymbol{a}}^{(r)}\right) \otimes \left(\boldsymbol{a} - \overline{\boldsymbol{a}}^{(r)}\right) \right\rangle^{(r)} = \langle \boldsymbol{a} \otimes \boldsymbol{a} \rangle^{(r)} - \overline{\boldsymbol{a}}^{(r)} \otimes \overline{\boldsymbol{a}}^{(r)}. \tag{10}$$

The trace along the fourth order tensor $\mathbb{K}$, where the tensor $\mathbb{K} = \mathbb{I} - \mathbb{J}$ stands for the deviatoric fourth-order isotropic projector, $\mathbb{I}$ being the symmetric fourth-order identity tensor and $\mathbb{J}$ the spherical fourth-order isotropic projector whose components are respectively $\mathbb{I}_{ijkl} = \frac{1}{2}(\delta_{ik}\delta_{jl} + \delta_{il}\delta_{jk})$ and $\mathbb{J}_{ijkl} = \frac{1}{3}\delta_{ij}\delta_{kl}$, quantifies in particular the fluctuations of the deviatoric part of the field $\boldsymbol{a}$:

$$\iota\, C^{(r)}(\boldsymbol{a}) :: \mathbb{K} = \left(\overline{\overline{a}}^{(r)}\right)^2 - \left(\overline{a}^{(r)}_{eq}\right)^2, \tag{11}$$

where $a_{eq} = \sqrt{\iota \boldsymbol{a}_d : \boldsymbol{a}_d}$ is the von Mises (stress or strain) equivalent of $\boldsymbol{a}$.
The RVE is submitted to a macroscopic strain loading history $\boldsymbol{E}(t)$. Therefore, the local problem to be solved reads

$$\left\{\begin{array}{l} \left.\begin{array}{l} \boldsymbol{\sigma} = \dfrac{\partial\, w}{\partial\, \boldsymbol{\varepsilon}}(\boldsymbol{\varepsilon}, \boldsymbol{\alpha}) \\ \dfrac{\partial\, w}{\partial\, \boldsymbol{\alpha}}(\boldsymbol{\varepsilon}, \boldsymbol{\alpha}) + \dfrac{\partial\, \varphi}{\partial\, \dot{\boldsymbol{\alpha}}}(\dot{\boldsymbol{\alpha}}, \boldsymbol{\alpha}) = 0 \\ \boldsymbol{\varepsilon} \text{ kinematically admissible (K.A.)} \\ \text{div}(\boldsymbol{\sigma}) = 0 \end{array}\right\} \forall (\underline{x}, t) \in \Omega \times [0, T] \\ \langle \boldsymbol{\varepsilon}(t) \rangle = \boldsymbol{E}(t)\ \forall t \in [0, T] \text{ + B.C. on } \partial\Omega \end{array}\right. \tag{12}$$

In the sequel, it is implicitly assumed that affine displacement boundary conditions (B.C.), i.e. $\underline{u} = \boldsymbol{E}(t).\underline{x}$, are applied on $\partial\Omega$ where $\underline{u}$ is the local displacement field from which the K.A. strain field is derived. In fact, all B.C. satisfying the macro-homogeneity relation, i.e. the validity of Hill's relation $\langle \boldsymbol{\sigma} : \boldsymbol{\varepsilon} \rangle = \langle \boldsymbol{\sigma} \rangle : \langle \boldsymbol{\varepsilon} \rangle$, would also be suitable for the problem addressed in this paper.
Approximating Eq. $(12)_2$ by Eq. (7) and making use of Eq. (8) induced by the variational problem (5), the time discretization procedure applied to Eq. (12) leads

to the following discretized version of the local problem, at time $t_{n+1}$, assuming the solution at time $t_n$ to be known, and in particular the field of internal variables $\boldsymbol{\alpha}_n$:

$$\left\{\begin{array}{l} \left.\begin{array}{l} \boldsymbol{\sigma} = \dfrac{\partial\, w_\Delta}{\partial\, \boldsymbol{\varepsilon}}(\boldsymbol{\varepsilon}, \boldsymbol{\alpha}_n) \\ \boldsymbol{\varepsilon} \text{ K.A.} \\ \text{div}(\boldsymbol{\sigma}) = 0 \end{array}\right\} \forall \underline{x} \in \Omega \\ \langle \boldsymbol{\varepsilon} \rangle = \boldsymbol{E} \text{ + B.C. on } \partial\Omega, \end{array}\right. \tag{13}$$

where the local condensed incremental potential $w_\Delta$ and incremental potential $J$ are defined $\forall \underline{x} \in \Omega$ by

$$\left\{\begin{array}{l} w_\Delta\left(\underline{x}, \boldsymbol{\varepsilon}, \boldsymbol{\alpha}_n\right) = \inf\limits_{\boldsymbol{\alpha}} J(\underline{x}, \boldsymbol{\varepsilon}, \boldsymbol{\alpha}, \boldsymbol{\alpha}_n) \quad \text{with} \\ J(\underline{x}, \boldsymbol{\varepsilon}, \boldsymbol{\alpha}, \boldsymbol{\alpha}_n) = \displaystyle\sum_{r=1}^{N} J^{(r)}(\boldsymbol{\varepsilon}, \boldsymbol{\alpha}, \boldsymbol{\alpha}_n)\, \chi^r(\underline{x}) \quad \text{and} \\ J^{(r)}(\boldsymbol{\varepsilon}, \boldsymbol{\alpha}, \boldsymbol{\alpha}_n) = w^{(r)}(\boldsymbol{\varepsilon}, \boldsymbol{\alpha}) + \Delta t\, \varphi^{(r)}\left(\dfrac{\boldsymbol{\alpha} - \boldsymbol{\alpha}_n}{\Delta t}, \boldsymbol{\alpha}_n\right). \end{array}\right. \tag{14}$$

Accordingly, the solution $\boldsymbol{\varepsilon}_{n+1}$ of the local discretized problem (13) is also solution of the following minimum potential energy principle

$$\inf_{\boldsymbol{\varepsilon} \text{ K.A.}/\langle \boldsymbol{\varepsilon} \rangle = \boldsymbol{E}} \langle w_\Delta(\boldsymbol{\varepsilon}, \boldsymbol{\alpha}_n) \rangle = \inf_{\boldsymbol{\varepsilon} \text{ K.A.}/\langle \boldsymbol{\varepsilon} \rangle = \boldsymbol{E}} \langle \inf_{\boldsymbol{\alpha}} J(\boldsymbol{\varepsilon}, \boldsymbol{\alpha}, \boldsymbol{\alpha}_n) \rangle. \tag{15}$$

Defining the effective condensed incremental potential by

$$\tilde{w}_\Delta(\boldsymbol{E}, \boldsymbol{\alpha}_n) = \inf_{\boldsymbol{\varepsilon} \text{ K.A.}/\langle \boldsymbol{\varepsilon} \rangle = \boldsymbol{E}} \langle w_\Delta(\boldsymbol{\varepsilon}, \boldsymbol{\alpha}_n) \rangle, \tag{16}$$

and following Lahellec and Suquet [2], it is easily shown, thanks to relation $(13)_1$ and Hill's lemma, that the effective stress $\boldsymbol{\Sigma} = \langle \boldsymbol{\sigma} \rangle$ is given by[2]

$$\boldsymbol{\Sigma} = \frac{\partial \tilde{w}_\Delta}{\partial \boldsymbol{E}}(\boldsymbol{E}, \boldsymbol{\alpha}_n). \tag{17}$$

This provides the macroscopic stress $\boldsymbol{\Sigma}$ at time $t_{n+1}$ due to the prescribed strain $\boldsymbol{E}$. The variational definition (16) also provides the associated local strain field $\boldsymbol{\varepsilon}$ in $\Omega$. The local variational definition of the condensed incremental potential (14) finally provides the field of internal variables $\boldsymbol{\alpha}$, i.e. $\boldsymbol{\alpha}_{n+1}$. This allows to proceed to the next time step of the loading history.

## 3. Elastoplasticity with nonlinear kinematic hardening: the modified Chaboche model

The aim of this section is to present the constitutive law that will be adopted for the mechanical behavior of the phases exhibiting nonlinear kinematic hardening and implemented in the incremental variational principles developed in Section 2, on which the DIV formulation described in Section 4 relies.

The Armstrong-Frederick (AF) model [4] (see also [25]) is acknowledged for its capability to satisfactorily describe the nonlinear kinematic hardening of metals and the Bauschinger effect observed during cyclic loadings. This model has been formalized and popularised by Chaboche [5, 26] in the framework of non-associated plasticity. Accordingly, it does not belong to the framework of GSM and therefore cannot be implemented in the incremental variational principles de-

[2] In this relation, in agreement with the simplification previously adopted and concerning index $(n+1)$, $\boldsymbol{\Sigma} \equiv \boldsymbol{\Sigma}_{n+1}$ and $\boldsymbol{E} \equiv \boldsymbol{E}_{n+1}$.

scribed in Section 2. For this reason, and in order to make use of the incremental variational principles with the objective to extend the DIV to nonlinear kinematic hardening, we consider the modified Chaboche model [6] which is an approximation of the Armstrong Frederick model within the framework of materials whose behavior derives from two thermodynamic potentials.

To built this modified model, Chaboche [6] made use of the following free energy function

$$w^{(r)}\left(\boldsymbol{\varepsilon}, \boldsymbol{\varepsilon}^p, \boldsymbol{\beta}, p\right) = \frac{1}{2}\left(\boldsymbol{\varepsilon} - \boldsymbol{\varepsilon}^p\right) : \mathbb{L}^{(r)} : \left(\boldsymbol{\varepsilon} - \boldsymbol{\varepsilon}^p\right) + \frac{1}{2} a^{(r)} \boldsymbol{\beta} : \boldsymbol{\beta} + \widehat{w}^{(r)}(p), \quad (18)$$

in which $\boldsymbol{\varepsilon}$ and $\boldsymbol{\varepsilon}^p$ are the strain and plastic strain tensors, $\boldsymbol{\beta}$ the second-order dimensionless tensor, considered as a strain, standing for the kinematic hardening variable and $p$ the cumulative plastic deformation describing the isotropic hardening. Tensors $\boldsymbol{\varepsilon}^p$ and $\boldsymbol{\beta}$ are assumed both traceless. $\mathbb{L}^{(r)}$ is the tensor of elastic moduli, $a^{(r)}$ the kinematic hardening parameter and $\widehat{w}^{(r)}$ a scalar function which represents the stored energy associated with the isotropic hardening. As a second component of the modified Chaboche model, the classical Von Mises yield function is modified by adding the last term in the following expression

$$F^{(r)}(\boldsymbol{\sigma}, \boldsymbol{X}, R, \boldsymbol{\beta}) = (\sigma - X)_{eq} - \sigma_y^{(r)} - R^{(r)}(p) + \frac{1}{2}\frac{\gamma^{(r)}}{a^{(r)}}\left(\boldsymbol{X} : \boldsymbol{X} - \left(a^{(r)}\right)^2 \boldsymbol{\beta} : \boldsymbol{\beta}\right), \quad (19)$$

where $\boldsymbol{X}$ is the so-called back-stress. Accordingly, the classical evolution laws of the Armstrong-Frederick model can be retrieved by the normality rule. In particular, its nonlinear kinematic hardening law reads

$$\dot{\boldsymbol{\beta}} = \dot{\boldsymbol{\varepsilon}}^p - \frac{\gamma^{(r)}}{a^{(r)}} \boldsymbol{X}\, \dot{\varepsilon}_{eq}^p. \quad (20)$$

The definition (19) indicates that the yield function of this model depends not only on the thermodynamical "forces" $\boldsymbol{\sigma}$, $\boldsymbol{X}$ and $R$ but also on the state variable $\boldsymbol{\beta}$. It should be noted that the incorporation of the state law $\boldsymbol{X} = a^{(r)}\boldsymbol{\beta}$ into (19) allows to cancel the last term of this expression and thus to retrieve the Von Mises plastic yield function of the Armstrong-Frederick model.

The modified Chaboche model is thus defined by two potentials, its free energy $w^{(r)}$ given by (18) and its dual dissipation potential $\varphi^{*\,(r)}$ derived from the yield function (19) as

$$\varphi^{*\,(r)}\left(\boldsymbol{\sigma}, \boldsymbol{X}, R, \boldsymbol{\beta}\right) = \Phi_{\mathcal{C}_{F_\beta}}\left(\boldsymbol{\sigma}, \boldsymbol{X}, R, \boldsymbol{\beta}\right), \tag{21}$$

where $\Phi_{\mathcal{C}_{F_\beta}}$ denotes the indicator function of the convex set $\mathcal{C}_{F_\beta}$ defined by

$$\mathcal{C}_{F_\beta} = \left\{\left(\boldsymbol{\sigma}, \boldsymbol{X}, R, \boldsymbol{\beta}\right) / F\left(\boldsymbol{\sigma}, \boldsymbol{X}, R, \boldsymbol{\beta}\right) \leq 0\right\}. \tag{22}$$

As requested by our variational formulation, we now seek to determine the primal dissipation potential $\varphi^{(r)}$ which is the Legendre-Fenchel transform of the dual potential $\varphi^{*\,(r)}$ of the modified Chaboche model. In fact, such a dissipation potential has already been calculated by Bouby et al. [27] for the case where the last term $\frac{1}{2}\gamma^{(r)}a^{(r)}\boldsymbol{\beta} : \boldsymbol{\beta}$ in (19) is missing. The same expression associated now with the modified Chaboche model for which the last term $\frac{1}{2}\,a^{(r)}\,\gamma^{(r)}\boldsymbol{\beta} : \boldsymbol{\beta}$ in Eq. (19) is accounted for, can be easily derived from the result of Bouby et al. [27] by replacing the initial plasticity threshold $\sigma_y^{(r)}$ by an equivalent plasticity threshold $\tilde{\sigma}_y^{(r)} = \sigma_y^{(r)} + \frac{3}{4}\,a^{(r)}\gamma^{(r)}\beta_{eq}^2$. Accordingly, one gets

$$\varphi^{(r)}\left(\dot{\boldsymbol{\varepsilon}}^p, \dot{\boldsymbol{\beta}}, \dot{p}, \boldsymbol{\beta}\right) = \phi^{(r)}\left(\dot{\boldsymbol{\varepsilon}}^p, \dot{\boldsymbol{\beta}}, \boldsymbol{\beta}\right) + \Phi_{\mathcal{C}}\left(\dot{\boldsymbol{\varepsilon}}^p, \dot{p}\right), \tag{23}$$

with

$$\phi^{(r)}\left(\dot{\boldsymbol{\varepsilon}}^p,\dot{\boldsymbol{\beta}},\boldsymbol{\beta}\right)=\begin{cases}\phi_1^{(r)}\left(\dot{\boldsymbol{\varepsilon}}^p,\dot{\boldsymbol{\beta}},\boldsymbol{\beta}\right) & \text{if } \left(\dot{\varepsilon}^p-\dot{\beta}\right)_{eq}\leq\dot{\varepsilon}^p_{eq}\sqrt{\frac{4}{3}\frac{\gamma^{(r)}}{a^{(r)}}\left(\sigma_y^{(r)}+\frac{3}{4}\,a^{(r)}\gamma^{(r)}\,\beta^2_{eq}\right)}\\ \phi_2^{(r)}\left(\dot{\boldsymbol{\varepsilon}}^p,\dot{\boldsymbol{\beta}},\boldsymbol{\beta}\right) & \text{otherwise,}\end{cases}\tag{24}$$

where

$$\begin{aligned}\phi_1^{(r)}\left(\dot{\boldsymbol{\varepsilon}}^p,\dot{\boldsymbol{\beta}},\boldsymbol{\beta}\right)&=\left(\sigma_y^{(r)}+\frac{3}{4}\,a^{(r)}\gamma^{(r)}\,\beta^2_{eq}\right)\dot{\varepsilon}^p_{eq}+\frac{3}{4}\frac{a^{(r)}}{\gamma^{(r)}}\frac{\left(\dot{\varepsilon}^p-\dot{\beta}\right)^2_{eq}}{\dot{\varepsilon}^p_{eq}}\\ \phi_2^{(r)}\left(\dot{\boldsymbol{\varepsilon}}^p,\dot{\boldsymbol{\beta}},\boldsymbol{\beta}\right)&=\left(\dot{\varepsilon}^p-\dot{\beta}\right)_{eq}\sqrt{3\,\frac{a^{(r)}}{\gamma^{(r)}}\left(\sigma_y^{(r)}+\frac{3}{4}\,a^{(r)}\gamma^{(r)}\,\beta^2_{eq}\right)},\end{aligned}\tag{25}$$

and

$$\Phi_{\mathcal{C}}(\dot{\boldsymbol{\varepsilon}}^p,\dot{p})=\begin{cases}0 & \text{if } (\dot{\boldsymbol{\varepsilon}}^p,\dot{p})\in\mathcal{C}\\ +\infty & \text{otherwise,}\end{cases}\tag{26}$$

the indicator function of the convex set $\mathcal{C}$ defined by

$$\mathcal{C}=\left\{(\dot{\boldsymbol{\varepsilon}}^p,\dot{p})\,/\,g(\dot{\boldsymbol{\varepsilon}}^p,\dot{p})=\dot{\varepsilon}^p_{eq}-\dot{p}\leq 0\right\}.\tag{27}$$

Eventually, following Bouby et al. [27], it is easily checked that applying the evolution law $(2)_1$ to the first branch $\phi_1^{(r)}$ of the dissipation potential for $\dot{\boldsymbol{\alpha}}\neq 0$ leads to the evolution laws of the Armstrong-Frederick model together with the fact that the thermodynamical forces belong to the plastic loading regime, i.e. $F^{(r)}(\boldsymbol{\sigma},\boldsymbol{X},R,\boldsymbol{\beta})=0$ with $F^{(r)}$ defined by Eq. (19). For $\dot{\boldsymbol{\alpha}}=\mathbf{0}$, $\boldsymbol{\mathcal{A}}_\alpha\in\partial_{\dot{\boldsymbol{\alpha}}}\phi_1(\dot{\boldsymbol{\alpha}}=0)$. Bouby et al. [27] showed that this subdifferential corresponds to the elastic domain $F^{(r)}(\boldsymbol{\sigma},\boldsymbol{X},R,\boldsymbol{\beta})<0$. Lastly, the evolution law $(2)_1$ applied

to the second branch $\phi_2^{(r)}$ leads to the following equation

$$\boldsymbol{\sigma}_d = \boldsymbol{X} = \frac{2}{3}\sqrt{3\,\frac{a^{(r)}}{\gamma^{(r)}}\left(\sigma_y^{(r)} + \frac{3}{4}\,a^{(r)}\gamma^{(r)}\beta_{eq}^2\right)}\,\frac{\dot{\boldsymbol{\varepsilon}}^p - \dot{\boldsymbol{\beta}}}{\left(\dot{\varepsilon}^p - \dot{\beta}\right)_{eq}} \quad \text{for } \dot{\boldsymbol{\varepsilon}}^p \neq \dot{\boldsymbol{\beta}}, \quad (28)$$

where, as shown by Bouby et al. [27], the points $\boldsymbol{\sigma}_d = \boldsymbol{X}$ belong to the surface of plasticity $F^{(r)}(\boldsymbol{\sigma}, \boldsymbol{X}, R, \boldsymbol{\beta}) = 0$.

## 4. Extension of the DIV formulation to elastoplastic composites with both isotropic and nonlinear kinematic hardening

We now aim to extend the DIV formulation [1], initially developed for elastoplastic composites with isotropic and linear kinematic hardening, to the case of nonlinear kinematic hardening. The DIV procedure relies on a key idea proposed by Agoras et al. [3], which consists in addressing sequentially, first the linearization of the local behavior and then the uniformization of the resulting LCC which exhibits a heterogeneous polarization inside the phases. For that, the variational procedure of Ponte Castañeda [7] is applied twice: once to linearize the local behavior and a second time to approximate the resulting heterogeneous LCC by a different one with now homogeneous intraphase properties. Since a lot of the calculations used in this extension are shared with those already presented in [1] for the case of isotropic and linear kinematic hardening, we only present in details the new calculations and sketch, for the sake of conciseness, the calculations already detailed in [1].

*4.1. Local behavior*

The behavior of the phases is governed by the Modified Chaboche model (presented in Section 3) whose constitutive relations are defined by means of two potentials: the free-energy potential given by (18) and the dissipation potential defined by (23), (24), (25). In view of applying the incremental variational principles presented in Section (2), for the sake of simplicity we make the following choice.

**Assumption 1.** *In the sequel, we only consider the first branch $\phi_1^{(r)}$ of the dissipation potential to describe the dissipative part of the local behavior of the phases.*

This choice, which consists to drop the branch $\phi_2^{(r)}$, amounts to exclude the possibility to reach the particular stress states ($\boldsymbol{\sigma}_d = \boldsymbol{X}$) of the surface of plasticity.

In order to simplify the calculations, let us introduce the following change of variable

$$\boldsymbol{\nu} = \boldsymbol{\beta} - \boldsymbol{\varepsilon}^p, \tag{29}$$

such that the internal variables now read $\boldsymbol{\alpha} = (\boldsymbol{\varepsilon}^p, \boldsymbol{\nu}, p)$. With these new notations, one has

- the free-energy

$$w^{(r)}(\boldsymbol{\varepsilon}, \boldsymbol{\varepsilon}^p, \boldsymbol{\nu}, p) = \frac{1}{2}\left(\boldsymbol{\varepsilon} - \boldsymbol{\varepsilon}^p\right) : \mathbb{L}^{(r)} : \left(\boldsymbol{\varepsilon} - \boldsymbol{\varepsilon}^p\right) + \frac{1}{2} a^{(r)}\left(\boldsymbol{\nu} + \boldsymbol{\varepsilon}^p\right) : \left(\boldsymbol{\nu} + \boldsymbol{\varepsilon}^p\right) + \widehat{w}^{(r)}(p), \tag{30}$$

- the dissipation potential

$$\varphi^{(r)}\left(\dot{\boldsymbol{\varepsilon}}^p, \dot{\boldsymbol{\nu}}, \dot{p}, \boldsymbol{\varepsilon}^p, \boldsymbol{\nu}\right) = \phi^{(r)}\left(\dot{\varepsilon}^p_{eq}, \dot{\nu}_{eq}, \boldsymbol{\varepsilon}^p, \boldsymbol{\nu}\right) + \Phi_{\mathcal{C}}\left(\dot{\boldsymbol{\varepsilon}}^p, \dot{p}\right), \tag{31}$$

with

$$\begin{aligned}&\phi^{(r)}\left(\dot{\varepsilon}^p_{eq},\dot{\nu}_{eq},\boldsymbol{\varepsilon}^p,\boldsymbol{\nu}\right)=\phi^{(r)}_1\left(\dot{\varepsilon}^p_{eq},\dot{\nu}_{eq},\boldsymbol{\varepsilon}^p,\boldsymbol{\nu}\right)\\&\text{if }\ \dot{\nu}_{eq}\leq\dot{\varepsilon}_{eq}\sqrt{\frac{4}{3}\frac{\gamma^{(r)}}{a^{(r)}}\left(\sigma_y^{(r)}+\frac{3}{4}\,a^{(r)}\gamma^{(r)}\left(\varepsilon^p+\nu\right)^2_{eq}\right)},\end{aligned}\tag{32}$$

and

$$\phi^{(r)}_1\left(\dot{\varepsilon}^p_{eq},\dot{\nu}_{eq},\boldsymbol{\varepsilon}^p,\boldsymbol{\nu}\right)=\left(\sigma_y^{(r)}+\frac{3}{4}\,a^{(r)}\gamma^{(r)}\left(\nu+\varepsilon^p\right)^2_{eq}\right)\dot{\varepsilon}^p_{eq}+\frac{3}{4}\,\frac{a^{(r)}}{\gamma^{(r)}}\,\frac{\dot{\nu}^2_{eq}}{\dot{\varepsilon}^p_{eq}},\tag{33}$$

The stress tensor and the irreversible thermodynamic forces read

$$\begin{cases}\boldsymbol{\sigma}=\dfrac{\partial w^{(r)}}{\partial\boldsymbol{\varepsilon}}(\boldsymbol{\varepsilon},\boldsymbol{\varepsilon}^p,\boldsymbol{\nu},p)=\mathbb{L}^{(r)}:(\boldsymbol{\varepsilon}-\boldsymbol{\varepsilon}^p)\\\boldsymbol{A}_\nu=-\dfrac{\partial w^{(r)}}{\partial\boldsymbol{\nu}}(\boldsymbol{\varepsilon},\boldsymbol{\varepsilon}^p,\boldsymbol{\nu},p)=-a^{(r)}(\boldsymbol{\nu}+\boldsymbol{\varepsilon}^p)=-\boldsymbol{X}\\\boldsymbol{A}_{\varepsilon^p}=-\dfrac{\partial w^{(r)}}{\partial\boldsymbol{\varepsilon}^p}(\boldsymbol{\varepsilon},\boldsymbol{\varepsilon}^p,\boldsymbol{\nu},p)=\mathbb{K}:\mathbb{L}^{(r)}:(\boldsymbol{\varepsilon}-\boldsymbol{\varepsilon}^p)-a^{(r)}(\boldsymbol{\nu}+\boldsymbol{\varepsilon}^p)=\boldsymbol{\sigma}_d-\boldsymbol{X}\\A_p=-\dfrac{\partial w^{(r)}}{\partial\,p}(\boldsymbol{\varepsilon},\boldsymbol{\varepsilon}^p,\boldsymbol{\nu},p)=-R^{(r)}(p).\end{cases}\tag{34}$$

The evolution laws are obtained by $\boldsymbol{A}_\alpha=\frac{\partial\varphi^{(r)}}{\partial\dot{\boldsymbol{\alpha}}}(\dot{\boldsymbol{\alpha}},\boldsymbol{\alpha})$. The yield function can be also rewritten as

$$\begin{aligned}F^{(r)}\left(\boldsymbol{\sigma},\boldsymbol{X},R,\boldsymbol{\varepsilon}^p,\boldsymbol{\nu}\right)=&(\sigma-X)_{eq}-\sigma_y^{(r)}-R^{(r)}(p)+\frac{1}{2}\frac{\gamma^{(r)}}{a^{(r)}}\boldsymbol{X}:\boldsymbol{X}\\&-\frac{1}{2}a^{(r)}\gamma^{(r)}\ \left(\boldsymbol{\nu}+\boldsymbol{\varepsilon}^p\right):\left(\boldsymbol{\nu}+\boldsymbol{\varepsilon}^p\right),\end{aligned}\tag{35}$$

### *4.2. Linearization of the local behavior*

To linearize the local behavior now described by the incremental potential $J$ defined by $(14)_{2,3}$ associated with (30) and (31), we introduce a linearized in-

cremental potential $J_L$ in which the dissipation potential $\varphi^{(r)}$ is approached by a quadratic function of $\dot{\boldsymbol{\varepsilon}}^p$ and $\dot{\boldsymbol{\nu}}$ which depends on viscosities $\eta_{\varepsilon^p}^{(r)}$ and $\eta_\nu^{(r)}$ chosen to be uniform over phase $r$

$$\begin{cases} J_L\left(\underline{x}, \boldsymbol{\varepsilon}, \boldsymbol{\varepsilon}^p, \boldsymbol{\nu}, \{\eta\}\right) = \displaystyle\sum_{r=1}^{N} J_L^{(r)}\left(\underline{x}, \boldsymbol{\varepsilon}, \boldsymbol{\varepsilon}^p, \boldsymbol{\nu}, \eta^{(r)}\right)\, \chi^{(r)}(\underline{x}) \quad \text{with} \\ J_L^{(r)}\left(\underline{x}, \boldsymbol{\varepsilon}, \boldsymbol{\varepsilon}^p, \boldsymbol{\nu}, \eta^{(r)}\right) = w^{(r)}(\boldsymbol{\varepsilon}, \boldsymbol{\varepsilon}^p, \boldsymbol{\nu}, p) - \widehat{w}^{(r)}(p) + \dfrac{\eta_{\varepsilon^p}^{(r)}}{\Delta t}(\boldsymbol{\varepsilon}^p - \boldsymbol{\varepsilon}_n^p) : (\boldsymbol{\varepsilon}^p - \boldsymbol{\varepsilon}_n^p) \\ \qquad\qquad + \dfrac{\eta_\nu^{(r)}}{\Delta t}(\boldsymbol{\nu} - \boldsymbol{\nu}_n) : (\boldsymbol{\nu} - \boldsymbol{\nu}_n), \end{cases} \tag{36}$$

with $\{\eta\} = \{\eta_{\varepsilon^p}\} \cup \{\eta_\nu\}$ where the notations $\{\eta_{\varepsilon^p}\}$ and $\{\eta_\nu\}$ stand for the sets $\{\eta_{\varepsilon^p}^{(1)}, ..., \eta_{\varepsilon^p}^{(N)}\}$ and $\{\eta_\nu^{(1)}, ..., \eta_\nu^{(N)}\}$, respectively. Furthermore, let us denote $\eta^{(r)} = \left(\eta_{\varepsilon^p}^{(r)}, \eta_\nu^{(r)}\right)$. In Eq. (36), the dependence w.r.t. $\underline{x}$ of $J_L^{(r)}$ refers to the dependence of this potential w.r.t. the fields of internal variables $\boldsymbol{\varepsilon}_n^p(\underline{x})$ and $\boldsymbol{\nu}_n(\underline{x})$. This new notation is adopted for ease of reading and will also apply in the sequel to other quantities that depend on the fields of internal variables a time $t_n$.

#### *4.2.1. General form of the proposed estimate of the effective incremental condensed potential*

To proceed with the linearization stage, we make use of the key idea of the variational procedure of Ponte Castañeda [7] which consists in rewriting the incremental potential as the sum of two terms $J = J_L + \Delta J$ such that the first term can be easily homogenized due to its quadratic form and the second one can still be evaluated. Accordingly, making use of the definition $(14)_{2,3}$ of $J$ and (31) of $\varphi^{(r)}$, we obtain

$$J^{(r)}\left(\underline{x}, \boldsymbol{\varepsilon}, \boldsymbol{\varepsilon}^p, \boldsymbol{\nu}, p, \eta^{(r)}\right) = J_L^{(r)}\left(\underline{x}, \boldsymbol{\varepsilon}, \boldsymbol{\varepsilon}^p, \boldsymbol{\nu}, \eta^{(r)}\right) + \Delta J^{(r)}\left(\underline{x}, \boldsymbol{\varepsilon}^p, \boldsymbol{\nu}, p, \eta^{(r)}\right), \tag{37}$$

with

$$\Delta J\left(\underline{x}, \boldsymbol{\varepsilon}^p, \boldsymbol{\nu}, p, \{\eta\}\right) = \sum_{r=1}^{N} \Delta J^{(r)}\left(\underline{x}, \boldsymbol{\varepsilon}^p, \boldsymbol{\nu}, p, \eta^{(r)}\right)\, \chi^{(r)}(\underline{x}), \tag{38}$$

and

$$\begin{aligned}\Delta J^{(r)}\left(\underline{x}, \boldsymbol{\varepsilon}^p, \boldsymbol{\nu}, p, \eta^{(r)}\right) =& \Delta t\, \varphi^{(r)}\left(\frac{\boldsymbol{\varepsilon}^p - \boldsymbol{\varepsilon}^p_n}{\Delta t}, \frac{\boldsymbol{\nu} - \boldsymbol{\nu}_n}{\Delta t}, \frac{p - p_n}{\Delta t}, \left(\varepsilon^p_n + \nu_n\right)_{eq}\right) + \widehat{w}^{(r)}(p) \\ & - \frac{\eta^{(r)}_{\varepsilon^p}}{\Delta t}(\boldsymbol{\varepsilon}^p - \boldsymbol{\varepsilon}^p_n) : (\boldsymbol{\varepsilon}^p - \boldsymbol{\varepsilon}^p_n) - \frac{\eta^{(r)}_{\nu}}{\Delta t}(\boldsymbol{\nu} - \boldsymbol{\nu}_n) : (\boldsymbol{\nu} - \boldsymbol{\nu}_n).\end{aligned} \tag{39}$$

The term $\left(\varepsilon^p_n + \nu_n\right)_{eq}$ which appears in Eq. (39) results from the particular form (32) of the considered dissipation potential, as well as from the definition $(14)_3$ of $J^{(r)}$ in which the function $\varphi^{(r)}$ is evaluated at $(\dot{\boldsymbol{\alpha}}, \boldsymbol{\alpha}_n)$ and not at $(\dot{\boldsymbol{\alpha}}, \boldsymbol{\alpha})$, as seen above in Section 2.2. Regarding the latter, it is worth noting that the dependance of the dissipation potential with the internal variables $\boldsymbol{\varepsilon}^p$ and $\boldsymbol{\nu}$ is solely related to the term $\sigma_y^{(r)} + \frac{3}{4}a^{(r)}\gamma^{(r)}(\boldsymbol{\nu} + \boldsymbol{\varepsilon}^p)^2_{eq}$ which exhibits the regularity announced in Section 2.2.

In what follows, in order to obtain a closed-form homogenization model making use of overall per-phase quantities instead of details of local fields, we make use of the following mean-field type approximation

**Assumption 2.**

$$\varphi^{(r)}\left(\dot{\boldsymbol{\varepsilon}}^p, \dot{\boldsymbol{\nu}}, \dot{p}, \left(\varepsilon^p_n + \nu_n\right)_{eq}\right) \approx \varphi^{(r)}\left(\dot{\boldsymbol{\varepsilon}}^p, \dot{\boldsymbol{\nu}}, \dot{p}, \overline{\overline{\varepsilon^p_n + \nu_n}}^{(r)}\right). \tag{40}$$

In this expression, we replace the pointwise fluctuating variable $\left(\varepsilon^p_n + \nu_n\right)_{eq}$ by a constant reference value chosen to be its second-order moment over the phase. Although other choices would have been possible, the considered choice is inspired by the modified secant type approaches which have shown their efficiency

in the framework of nonlinear elasticity. Since $\overline{\overline{\varepsilon_n^p + \nu_n}}^{(r)}$ is known from the former step, for ease of notation, the quantity $\varphi^{(r)}\left(\dot{\boldsymbol{\varepsilon}}^p, \dot{\boldsymbol{\nu}}, \dot{p}, \overline{\overline{\varepsilon_n^p + \nu_n}}^{(r)}\right)$ will be denoted $\varphi^{(r)}\left(\dot{\boldsymbol{\varepsilon}}^p, \dot{\boldsymbol{\nu}}, \dot{p}\right)$ in the sequel.

Reporting the decomposition (37) of $J^{(r)}$ in the variational formulation (15), (16), one gets

$$\tilde{w}_\Delta(\boldsymbol{E}) = \inf_{\langle\boldsymbol{\varepsilon}\rangle=\boldsymbol{E}} \left\{ \inf_{(\boldsymbol{\varepsilon}^p,\boldsymbol{\nu},p)} \langle J_L\left(.,\boldsymbol{\varepsilon},\boldsymbol{\varepsilon}^p,\boldsymbol{\nu},\{\eta\}\right) + \Delta J\left(.,\boldsymbol{\varepsilon}^p,\boldsymbol{\nu},p,\{\eta\}\right)\rangle \right\}, \quad (41)$$

where $J_L$ and $\Delta J$ are given by Eq. (36) and Eqs. (38), (39), (40), respectively.

By making use of stationarity conditions under inequality constraints induced by the indicator function $\Phi_{\mathcal{C}}$ defined by (26) and after some cumbersome calculations detailed in AppendixA, an estimate of the effective condensed incremental potential is derived and given by the following expression[3]

$$\begin{aligned}
\tilde{w}_\Delta(\boldsymbol{E}) &\approx \tilde{w}_\Delta^{VAR}(\boldsymbol{E},\{\eta\}) \\
&= \inf_{\langle\boldsymbol{\varepsilon}\rangle=\boldsymbol{E}} \left\{ \begin{array}{l} \displaystyle\inf_{(\boldsymbol{\varepsilon}^p,\boldsymbol{\nu},p)\Big/ \substack{h_1^{(r)}(\boldsymbol{\varepsilon}^p,\boldsymbol{\nu})\leq 0 \\ g_1(\boldsymbol{\varepsilon}^p,p)\leq 0}} \langle J_L(.,\boldsymbol{\varepsilon},\boldsymbol{\varepsilon}^p,\boldsymbol{\nu},\{\eta\})\rangle \\ + \quad \left\langle \displaystyle\operatorname*{stat}_{(\dot{\boldsymbol{\varepsilon}}^p,\dot{\boldsymbol{\nu}},\dot{p})\Big/ \substack{h^{(r)}(\dot{\boldsymbol{\varepsilon}}^p,\dot{\boldsymbol{\nu}})\leq 0 \\ g(\dot{\boldsymbol{\varepsilon}}^p,\dot{p})\leq 0}} \Delta J_{bis}(.,\dot{\boldsymbol{\varepsilon}}^p,\dot{\boldsymbol{\nu}},\dot{p},\{\eta\}) \right\rangle \end{array} \right\}
\end{aligned} \quad (42)$$

with

$$\Delta J_{bis}(\underline{x},\dot{\boldsymbol{\varepsilon}}^p,\dot{\boldsymbol{\nu}},\dot{p},\eta^{(r)}) = \Delta J(\underline{x},\dot{\boldsymbol{\varepsilon}}^p,\dot{\boldsymbol{\nu}},\dot{p},\eta^{(r)}) - \Phi_{\mathcal{C}}\left(\dot{\boldsymbol{\varepsilon}}^p,\dot{p}\right). \quad (43)$$

The constraints $g$ and $h^{(r)}$ which appear in Eq. (42) are respectively defined by

[3]The dot in expressions like $\langle J_L\left(.,\boldsymbol{\varepsilon},\boldsymbol{\varepsilon}^p,\boldsymbol{\nu},\{\eta\}\right)\rangle$ refers to a dummy variable over which the integration is performed.

Eq. (27) and by

$$h^{(r)}\left(\dot{\boldsymbol{\varepsilon}}^p, \dot{\boldsymbol{\nu}}\right) = \dot{\nu}_{eq} - \dot{\varepsilon}_{eq}\sqrt{\frac{4}{3}\frac{\gamma^{(r)}}{a^{(r)}}\left(\sigma_y^{(r)} + \frac{3}{4}\,a^{(r)}\gamma^{(r)}\left(\overline{\overline{\varepsilon_n^p + \nu_n}}^{(r)}\right)^2\right)}, \tag{44}$$

while the two last constraints $g_1$ and $h_1^{(r)}$, which are simply a rewriting of $g$ and $h^{(r)}$ in a total formulation, are given by

$$\begin{aligned}
&h_1^{(r)}(\boldsymbol{\varepsilon}^p, \boldsymbol{\nu}) = (\boldsymbol{\nu} - \boldsymbol{\nu}_n) : (\boldsymbol{\nu} - \boldsymbol{\nu}_n) - \\
&(\boldsymbol{\varepsilon}^p - \boldsymbol{\varepsilon}_n^p) : (\boldsymbol{\varepsilon}^p - \boldsymbol{\varepsilon}_n^p)\left(\frac{4}{3}\frac{\gamma^{(r)}}{a^{(r)}}\left(\sigma_y^{(r)} + \frac{3}{4}\,a^{(r)}\gamma^{(r)}\left(\overline{\overline{\varepsilon_n^p + \nu_n}}^{(r)}\right)^2\right)\right) \\
&g_1(\boldsymbol{\varepsilon}^p, p) = (\boldsymbol{\varepsilon}^p - \boldsymbol{\varepsilon}_n^p) : (\boldsymbol{\varepsilon}^p - \boldsymbol{\varepsilon}_n^p) - \frac{3}{2}(p - p_n)^2.
\end{aligned} \tag{45}$$

It should be noted that the constraints $h_1^{(r)}(\boldsymbol{\varepsilon}^p, \boldsymbol{\nu})$ and $g_1(\boldsymbol{\varepsilon}^p, p)$ defined by Eq. (45) need to be satisfied $\forall \underline{x} \in \Omega^{(r)}$. Since $\boldsymbol{\varepsilon}_n^p$, $\boldsymbol{\nu}_n$ and $p_n$ are possibly heterogeneous fields over the RVE $\Omega$, the infimum problem in Eq. (42) is difficult to be solved in a mean-field homogenization framework. To overcome this difficulty, these constraints are relaxed by making use of the following mean-field type assumption.

**Assumption 3.** *The pointwise constraints* $h_1^{(r)}(\boldsymbol{\varepsilon}^p, \boldsymbol{\nu}) \leq 0$ *and* $g_1(\boldsymbol{\varepsilon}^p, p) \leq 0$ *are relaxed in Eq.* (42) *by the following* $2N$ *per-phase average conditions:* $\langle h_1^{(r)} \rangle^{(r)} \leq 0$ *and* $\langle g_1 \rangle^{(r)} \leq 0\ \forall r \in \{1, ..., N\}$.

Such a simplification is not required for the $\Delta J_{bis}$ term, for which the optimization can be performed separately and uniformly at all positions $\underline{x}$ in the RVE, and turns out to lead to per-phase uniform optimal quantities $f^{(r)}$, as detailed in Subsection 4.2.2. The variational estimate of the effective condensed potential

reads then

$$\tilde{w}_\Delta(\boldsymbol{E}) \approx \tilde{w}_\Delta^{VAR}(\boldsymbol{E},\{\eta\})$$
$$= \inf_{\langle\boldsymbol{\varepsilon}\rangle=\boldsymbol{E}} \left\{ \inf_{(\boldsymbol{\varepsilon}^p,\boldsymbol{\nu},p) \Big/ \substack{\langle h_1^{(r)}(\boldsymbol{\varepsilon}^p,\boldsymbol{\nu})\rangle^{(r)}\leq 0 \\ \langle g_1(\boldsymbol{\varepsilon}^p,p)\rangle^{(r)}\leq 0}} \langle J_L(.,\boldsymbol{\varepsilon},\boldsymbol{\varepsilon}^p,\boldsymbol{\nu},\{\eta\})\rangle \right\} + \Delta t \sum_{r=1}^{N} c^{(r)} f^{(r)}\left(\eta^{(r)}\right), \tag{46}$$

with

$$\Delta t \sum_{r=1}^{N} c^{(r)}\, f^{(r)}\left(\eta^{(r)}\right) = \left\langle \operatorname*{stat}_{(\dot{\boldsymbol{\varepsilon}}^p,\dot{\boldsymbol{\nu}},\dot{p}) \Big/ \substack{h^{(r)}(\dot{\boldsymbol{\varepsilon}}^p,\dot{\boldsymbol{\nu}})\leq 0 \\ g(\dot{\boldsymbol{\varepsilon}}^p,\dot{p})\leq 0}} \Delta J_{bis}(.,\dot{\boldsymbol{\varepsilon}}^p,\dot{\boldsymbol{\nu}},\dot{p},\{\eta\}) \right\rangle. \tag{47}$$

Eventually, a last optimization w.r.t. the set $\{\eta\}$ is performed, thus leading to the final DIV estimate of $\tilde{w}_\Delta$:

$$\tilde{w}_\Delta(\boldsymbol{E}) \approx \tilde{w}_\Delta^{DIV}(\boldsymbol{E}) = \operatorname*{stat}_{\{\eta\}} \tilde{w}_\Delta^{VAR}\left(\boldsymbol{E},\{\eta\}\right). \tag{48}$$

*4.2.2. Stationarity conditions*

The development of the various stationarity conditions of Eqs. (46), (47) and (48) leads to cumbersome calculations which, for reason of conciseness, are not reported in this paper. In essence, it consists in derivations similar to those reported in the former version of this model dealing with linear kinematic hardening [1] with the difference that now an additional internal variable, namely $\boldsymbol{\nu}$, is introduced and the optimization is performed under two sets of constraints instead of one. The reader interested by this issue is referred to the work of Lucchetta [28] where the whole details of the calculations are reported. The results are as follows. It is shown that the stationarity conditions of $\Delta J_{bis}$ w.r.t. the local rate of

the internal variables and of $\tilde{w}_\Delta^{VAR}$ w.r.t. $\eta^{(r)}$ provide the following expressions of the viscosities $\eta_{\varepsilon^p}^{(r)}$ and $\eta_\nu^{(r)}$, which depend on the second order moments $\overline{\overline{\dot{\varepsilon}^p}}^{(r)}$ and $\overline{\overline{\dot{\nu}}}^{(r)}$, and the one of the cumulated plastic strain $p^{(r)}$ which is uniform per phase and also depends on $\overline{\overline{\dot{\varepsilon}^p}}^{(r)}$

$$\begin{aligned}
\eta_{\varepsilon^p}^{(r)} &= \frac{\sigma_y^{(r)} + R^{(r)}\left(p^{(r)}\right) - \frac{3\,a^{(r)}}{4\,\gamma^{(r)}}\left(\frac{\overline{\overline{\dot{\nu}}}^{(r)}}{\overline{\overline{\dot{\varepsilon}^p}}^{(r)}}\right)^2 + \frac{3}{4}\,a^{(r)}\gamma^{(r)}\left(\overline{\overline{\nu_n + \varepsilon_n^p}}^{(r)}\right)^2}{3\,\overline{\overline{\dot{\varepsilon}^p}}^{(r)}} \\
\eta_\nu^{(r)} &= \frac{a^{(r)}}{2\,\gamma^{(r)}\,\overline{\overline{\dot{\varepsilon}^p}}^{(r)}}, \quad \text{with} \quad p^{(r)} = p_n^{(r)} + \Delta t\,\overline{\overline{\dot{\varepsilon}^p}}^{(r)}.
\end{aligned} \tag{49}$$

Moreover, the stationarity conditions also provide the expression of the function $f^{(r)}$ defined by Eq. (47) as follows

$$\begin{aligned}
f^{(r)}\left(\eta_{\varepsilon^p}^{(r)}, \eta_\nu^{(r)}\right) &= \left(\sigma_y^{(r)} + \frac{3}{4}\,a^{(r)}\gamma^{(r)}\left(\overline{\overline{\nu_n + \varepsilon_n^p}}^{(r)}\right)^2\right)\overline{\overline{\dot{\varepsilon}^p}}\left(\eta_\nu^{(r)}\right) + \frac{3}{4}\,\frac{a^{(r)}}{\gamma^{(r)}}\,\frac{\left(\overline{\overline{\dot{\nu}}}\left(\eta^{(r)}\right)\right)^2}{\widehat{\dot{\varepsilon}^p}\left(\eta_\nu^{(r)}\right)} \\
&+ \frac{\hat{w}^{(r)}}{\Delta t}\left(p_n^{(r)} + \Delta t\,\overline{\overline{\dot{\varepsilon}^p}}^{(r)}\left(\eta_\nu^{(r)}\right)\right) - \frac{3}{2}\eta_{\varepsilon^p}^{(r)}\left(\overline{\overline{\dot{\varepsilon}^p}}^{(r)}\left(\eta_\nu^{(r)}\right)\right)^2 - \frac{3}{2}\eta_\nu^{(r)}\left(\overline{\overline{\dot{\nu}}}^{(r)}\left(\eta^{(r)}\right)\right)^2,
\end{aligned} \tag{50}$$

where the second-order moments $\overline{\overline{\dot{\varepsilon}^p}}^{(r)} = \overline{\overline{\dot{\varepsilon}^p}}^{(r)}\left(\eta_\nu^{(r)}\right)$ and $\overline{\overline{\dot{\nu}}}^{(r)} = \overline{\overline{\dot{\nu}}}^{(r)}\left(\eta^{(r)}\right)$ are two scalar functions which depend on $\eta_\nu^{(r)}$ and $\eta^{(r)} = \left(\eta_{\varepsilon^p}^{(r)}, \eta_\nu^{(r)}\right)$, respectively. Their closed-form expressions can be straightforwardly obtained by inverting Eq. (49).

From the stationarity of $J_L$ w.r.t. the internal variables, we get the expressions of $\boldsymbol{\varepsilon}^p$ and $\boldsymbol{\nu}$ which linearly depend on the local strain field $\boldsymbol{\varepsilon}$ as well as on their value

computed at the previous time step $t_n$

$$\boldsymbol{\varepsilon}^p = \left[\mathbb{K} : \mathbb{L}^{(r)} + \left(2\,\frac{\eta_{\varepsilon^p}^{(r)}}{\Delta t} + a_{NL}^{(r)}\right)\mathbb{K}\right]^{-1} : \left[\mathbb{K} : \mathbb{L}^{(r)} : \boldsymbol{\varepsilon} + 2\,\frac{\eta_{\varepsilon^p}^{(r)}}{\Delta t}\boldsymbol{\varepsilon}_n^p - a_{NL}^{(r)}\boldsymbol{\nu}_n\right], \tag{51}$$

$$\boldsymbol{\nu} = -\frac{a_{NL}^{(r)}\Delta t}{2\,\eta_\nu^{(r)}}\left[\mathbb{K} : \mathbb{L}^{(r)} + \left(2\,\frac{\eta_{\varepsilon^p}^{(r)}}{\Delta t} + a_{NL}^{(r)}\right)\mathbb{K}\right]^{-1} :$$
$$\left[\mathbb{K} : \mathbb{L}^{(r)} : \boldsymbol{\varepsilon} + 2\,\frac{\eta_{\varepsilon^p}^{(r)}}{\Delta t}\boldsymbol{\varepsilon}_n^p - 2\,\frac{\eta_\nu^{(r)}}{\Delta t\,a^{(r)}}\left(\left(2\,\frac{\eta_{\varepsilon^p}^{(r)}}{\Delta t} + a^{(r)}\right)\mathbb{K} + \mathbb{K} : \mathbb{L}^{(r)}\right) : \boldsymbol{\nu}_n\right], \tag{52}$$

with

$$a_{NL}^{(r)} = \frac{2\,\frac{\eta_\nu^{(r)}}{\Delta t}a^{(r)}}{2\,\frac{\eta_\nu^{(r)}}{\Delta t} + a^{(r)}}. \tag{53}$$

We note that this linear dependence of the optimal internal variables with the current strain field $\boldsymbol{\varepsilon}$ ensures that the optimization problem w.r.t. the strain field $\boldsymbol{\varepsilon}$ is a thermoelastic problem, which can be solved with a linear mean field scheme adapted to the microstructure of the composite. In addition to these equations, the stationarity of $J_L$ also provides the following local linear constitutive laws

$$\begin{cases} \boldsymbol{\sigma}_d - \boldsymbol{X} = 2\,\eta_{\varepsilon^p}^{(r)}\,\dot{\boldsymbol{\varepsilon}}^p \\ -\boldsymbol{X} = 2\,\eta_\nu^{(r)}\,\dot{\boldsymbol{\nu}}. \end{cases} \tag{54}$$

The optimal viscosities $\eta_{\varepsilon^p}^{(r)}$ and $\eta_\nu^{(r)}$, which are defined by Eq. (49), can be interpreted as the modified secant viscous moduli associated with the elastoplastic behavior with nonlinear kinematic and isotropic hardening and evaluated at the

second-order moments $\overline{\overline{\dot{\varepsilon}^p}}^{(r)}$ and $\overline{\overline{\dot{\nu}}}^{(r)}$. From (49) and (54), we deduce that

$$\begin{cases} \overline{\overline{\sigma - X}}^{(r)} = \sigma_y^{(r)} + R^{(r)}\left(p^{(r)}\right) - \dfrac{3}{4}\dfrac{a^{(r)}}{\gamma^{(r)}}\left(\dfrac{\overline{\dot{\nu}}^{(r)}}{\overline{\dot{\varepsilon}^p}^{(r)}}\right)^2 + \dfrac{3}{4}\,a^{(r)}\gamma^{(r)}\left(\overline{\overline{\nu_n + \varepsilon_n^p}}^{(r)}\right)^2 \\ \overline{X}^{(r)} = \dfrac{3\,a^{(r)}\,\overline{\dot{\nu}}^{(r)}}{2\,\gamma^{(r)}\,\overline{\dot{\varepsilon}^p}^{(r)}}, \end{cases} \tag{55}$$

Making use of Eqs. $(34)_2$ and $(55)_2$, the following equality is straightforwardly obtained

$$\frac{3}{2}\,a^{(r)}\,\overline{\overline{\varepsilon^p + \nu}}^{(r)} = \frac{3}{2}\,\frac{a^{(r)}}{\gamma^{(r)}}\,\frac{\overline{\dot{\nu}}^{(r)}}{\overline{\dot{\varepsilon}^p}^{(r)}}. \tag{56}$$

Reporting Eq. (56) in the definition $(49)_1$ of $\eta_{\varepsilon^p}^{(r)}$, we have

$$\eta_{\varepsilon^p}^{(r)} = \frac{\sigma_y^{(r)} + R^{(r)}\left(p_n^{(r)} + \Delta t\,\overline{\dot{\varepsilon}^p}^{(r)}\right) + \frac{3}{4}\,\gamma^{(r)}\,a^{(r)}\left[\left(\overline{\overline{\nu_n + \varepsilon_n^p}}^{(r)}\right)^2 - \left(\overline{\overline{\nu + \varepsilon^p}}^{(r)}\right)^2\right]}{3\,\overline{\dot{\varepsilon}^p}^{(r)}}. \tag{57}$$

When $\Delta t$ is small enough, the term $\frac{3}{4}\,\gamma^{(r)}\,a^{(r)}\left[\left(\overline{\overline{\nu_n + \varepsilon_n^p}}^{(r)}\right)^2 - \left(\overline{\overline{\nu + \varepsilon^p}}^{(r)}\right)^2\right]$ become negligible w.r.t. $\sigma_y^{(r)} + R^{(r)}\left(p_n^{(r)} + \Delta t\,\overline{\dot{\varepsilon}^p}^{(r)}\right)$ such that

$$\eta_{\varepsilon^p}^{(r)} = \frac{\sigma_y^{(r)} + R^{(r)}\left(p_n^{(r)} + \Delta t\,\overline{\dot{\varepsilon}^p}^{(r)}\right)}{3\,\overline{\dot{\varepsilon}^p}^{(r)}}. \tag{58}$$

Starting from Eq. $(55)_1$, the same procedure leads to the following equality for the plastic criterion of the DIV formulation

$$\overline{\overline{\sigma_d - X}}^{(r)} = \sigma_y^{(r)} + R^{(r)}\left(p^{(r)}\right). \tag{59}$$

Eq. (59) can be interpreted as the plastic yield function of the DIV formulation. It coincides with the local plastic yield function (35), for $X$ given by Eq. $(34)_2$, evaluated at the second-order moments of the local fields. Indeed, the local stress $(\sigma - X)_{eq}$ is approximated by $\overline{\overline{\sigma - X}}^{(r)}$ and the cumulated plastic deformation $p$ by $p^{(r)}$ whose evolution is given by the second-order moment of the plastic strain rate $\overline{\overline{\dot{\varepsilon}^p}}^{(r)}$ (see Eq. $(49)_3$).

*4.2.3. Determination of the LCC with heterogeneous intraphase polarization*

By reporting expressions (51), (52) of $\boldsymbol{\varepsilon}^p$ and $\boldsymbol{\nu}$ in the definition (36) of $J_L$, we obtain a thermoelastic LCC with per-phase free-energy $w_L^{(r)}$ defined as follows

$$\begin{aligned} w_L^{(r)}\left(\underline{x}, \boldsymbol{\varepsilon}, \eta^{(r)}\right) &= \inf_{(\boldsymbol{\varepsilon}^p, \boldsymbol{\nu}, p) \Big/ \substack{<h_1^{(r)}(\boldsymbol{\varepsilon}^p, \boldsymbol{\nu})>^{(r)} \leq 0 \\ <g_1(\boldsymbol{\varepsilon}^p, p)>^{(r)} \leq 0}} J_L^{(r)}\left(\underline{x}, \boldsymbol{\varepsilon}, \boldsymbol{\varepsilon}^p, \boldsymbol{\nu}, \eta^{(r)}\right) \\ &= \frac{1}{2}\,\boldsymbol{\varepsilon} : \mathbb{L}_L^{(r)} : \boldsymbol{\varepsilon} + \boldsymbol{\tau}_L^{(r)}(\underline{x}) : \boldsymbol{\varepsilon} + \frac{1}{2} f_L^{(r)}(\underline{x}), \end{aligned} \tag{60}$$

with

$$\begin{cases} \mathbb{L}_L^{(r)} = \mathbb{L}^{(r)} - \left[\mathbb{K} : \mathbb{L}^{(r)}\right] : \left[\mathbb{K} : \mathbb{L}^{(r)} + \left(2\,\dfrac{\eta_{\varepsilon^p}^{(r)}}{\Delta t} + a_{NL}^{(r)}\right)\mathbb{K}\right]^{-1} : \left[\mathbb{K} : \mathbb{L}^{(r)}\right] \\ \boldsymbol{\tau}_L^{(r)}(\underline{x}) = -\left[\mathbb{K} : \mathbb{L}^{(r)}\right] : \left[\mathbb{K} : \mathbb{L}^{(r)} + \left(2\,\dfrac{\eta_{\varepsilon^p}^{(r)}}{\Delta t} + a_{NL}^{(r)}\right)\mathbb{K}\right]^{-1} : \left[2\,\dfrac{\eta_{\varepsilon^p}^{(r)}}{\Delta t}\boldsymbol{\varepsilon}_n^p(\underline{x}) - a_{NL}^{(r)}\boldsymbol{\nu}_n(\underline{x})\right] \\ f_L^{(r)}(\underline{x}) = \left[\begin{array}{l} 2\,\dfrac{\eta_{\varepsilon^p}^{(r)}}{\Delta t}\boldsymbol{\varepsilon}_n^p(\underline{x}) : \mathbb{D}^{(r)} : \left(\mathbb{K} : \mathbb{L}^{(r)} + a_{NL}^{(r)}\mathbb{K}\right) : \boldsymbol{\varepsilon}_n^p(\underline{x}) \\ + a_{NL}^{(r)}\boldsymbol{\nu}_n(\underline{x}) : \mathbb{D}^{(r)} : \left(\mathbb{K} : \mathbb{L}^{(r)} + 2\,\dfrac{\eta_{\varepsilon^p}^{(r)}}{\Delta t}\mathbb{K}\right) : \boldsymbol{\nu}_n(\underline{x}) \\ + 4\,\dfrac{\eta_{\varepsilon^p}^{(r)}}{\Delta t}a_{NL}^{(r)}\boldsymbol{\varepsilon}_n^p(\underline{x}) : \mathbb{D}^{(r)} : \boldsymbol{\nu}_n(\underline{x}) \end{array}\right], \end{cases} \tag{61}$$

and

$$\mathbb{D}^{(r)} = \left[\mathbb{K} : \mathbb{L}^{(r)} + \left(2\,\frac{\eta_{\varepsilon^p}^{(r)}}{\Delta t} + a_{NL}^{(r)}\right)\mathbb{K}\right]^{-1} \tag{62}$$

It should be noted that the free-energy $w_L^{(r)}$ (Eq. (60)) corresponds to a LCC with heterogeneous intraphase properties. Though the local stiffness tensor $\mathbb{L}_L^{(r)}$ of this LCC is uniform in phase $r$, the polarization $\boldsymbol{\tau}_L^{(r)}$ and the scalar field $f_L^{(r)}$ depend on $\underline{x}$ through the heterogenous fields $\boldsymbol{\varepsilon}_n^p(\underline{x})$ and $\boldsymbol{\nu}_n(\underline{x})$. The effective energy of this LCC is defined by

$$\tilde{w}_L(\boldsymbol{E}, \{\eta\}) = \inf_{\langle\boldsymbol{\varepsilon}\rangle = \boldsymbol{E}} \langle w_L(., \boldsymbol{\varepsilon}, \{\eta\})\rangle. \tag{63}$$

From Eqs. (42), (48) and (50), we get[4]

$$\tilde{w}_\Delta(\boldsymbol{E}) \approx \tilde{w}_\Delta^{DIV}(\boldsymbol{E}) = \underset{\{\eta\}}{\text{stat}}\, \tilde{w}_\Delta^{VAR}(\boldsymbol{E}, \{\eta\}) = \tilde{w}_L(\boldsymbol{E}, \{\eta\}) + \Delta t \sum_{r=1}^{N} c^{(r)} f^{(r)} \left(\eta^{(r)}\right), \tag{64}$$

where $f^{(r)}$ is defined by Eq. (50). Finally, making use of the stationarity condition w.r.t. the viscosities $\eta^{(r)}$, we have

$$\boldsymbol{\Sigma} = \frac{\partial \tilde{w}_\Delta}{\partial \boldsymbol{E}}(\boldsymbol{E}) \approx \frac{\partial \tilde{w}_\Delta^{DIV}}{\partial \boldsymbol{E}}(\boldsymbol{E}) = \frac{\partial \tilde{w}_L}{\partial \boldsymbol{E}}(\boldsymbol{E}), \tag{65}$$

where $\tilde{w}_L(\boldsymbol{E})$ stands for the value of $\tilde{w}_L\left(\boldsymbol{E}, \{\eta\}\right)$ calculated for the optimal set $\{\eta\}$.

### *4.3. Uniformization of the local behavior*

#### *4.3.1. General procedure*

As mentioned in previous Section, the LCC of energy $w_L$ resulting from the linearization stage corresponds to a thermoelastic composite with heterogeneous intraphase polarization. Accordingly, its effective behavior cannot be obtained by classical linear mean-field homogenization schemes - even if it could be derived by costly full-field computations. In order to deal with the heterogeneity of the polarization, Lahellec et al. [29] presented an efficient method which relies on the variational procedure of Ponte Castañeda [7]. This method approximates the free-energy $w_L$ by an energy $w_0$ associated with a classical LCC with per-phase homogeneous polarization tensors $\boldsymbol{\tau}_0^{(r)}$ and tensors of moduli $\mathbb{L}_0^{(r)} \neq \mathbb{L}_L^{(r)}$ such that the effective behavior as well as the statistics of the fields in the composite

[4]Note that for the sake of simplicity the set $\{\eta\}$ in Eq. (64) represents both dummy variables in the third expression and the optimal values of the viscosities in the last one.

can now be evaluated by classical linear homogenization schemes. This idea has been implemented first by Agoras et al. [3] for viscoplastic composites without hardening and then by Lucchetta et al. [1] for elastoplastic composites with linear kinematic and isotropic hardening. In what follows, it is implemented for elastoplastic composites with nonlinear kinematic and isotropic hardening. Since its application to this behavior is similar to the case of elastoplastic composites with linear kinematic hardening, we only recall very briefly the main stages of the method and the reader is referred to [1] for the details of the calculations.

Making use of the key idea of the variational procedure of Ponte Castañeda [30], the energy $w_L^{(r)}$ can be rewritten as

$$w_L^{(r)}(\underline{x},\boldsymbol{\varepsilon}) = w_0^{(r)}(\boldsymbol{\varepsilon}) + \left[w_L^{(r)}(\underline{x},\boldsymbol{\varepsilon}) - w_0^{(r)}(\boldsymbol{\varepsilon})\right] = w_0^{(r)}(\boldsymbol{\varepsilon}) + \Delta w^{(r)}(\underline{x},\boldsymbol{\varepsilon}). \quad (66)$$

where $w_0$ corresponds to the energy of a classical thermoelastic LCC with homogeneous intraphase polarizations defined by

$$w_0(\underline{x},\boldsymbol{\varepsilon}) = \sum_{r=1}^{N} w_0^{(r)}(\boldsymbol{\varepsilon})\,\chi^{(r)}(\underline{x}), \quad \text{with} \quad w_0^{(r)}(\boldsymbol{\varepsilon}) = \frac{1}{2}\boldsymbol{\varepsilon} : \mathbb{L}_0^{(r)} : \boldsymbol{\varepsilon} + \boldsymbol{\tau}_0^{(r)} : \boldsymbol{\varepsilon} + \frac{1}{2} f_0^{(r)}. \quad (67)$$

Applying the procedure of Lahellec et al. [29] (see [1]), an estimate of the effective energy $\tilde{w}_L(\boldsymbol{E})$ can be derived and is given by the following expression

$$\tilde{w}_L(\boldsymbol{E}) = \underset{\mathbb{L}_0^{(r)},\boldsymbol{\tau}_0^{(r)},f_0^{(r)}}{\text{stat}} \left\{ \tilde{w}_0(\boldsymbol{E}) - \frac{1}{2}\sum_{r=1}^{N} c^{(r)} \left[ \left\langle \Delta\boldsymbol{\tau}^{(r)}(.) : \left(\Delta\mathbb{L}^{(r)}\right)^{-1} : \Delta\boldsymbol{\tau}^{(r)}(.) - \Delta f^{(r)}(.) \right\rangle^{(r)} \right] \right\}, \quad (68)$$

with

$$\tilde{w}_0(\boldsymbol{E}) = \inf_{\langle\boldsymbol{\varepsilon}\rangle=\boldsymbol{E}} \langle w_0(\boldsymbol{\varepsilon})\rangle\,. \quad (69)$$

In Eq. (68), use has been made of the notation $\Delta a^{(r)}(.) = a_L^{(r)}(.) - a_0^{(r)}$, e.g. $\Delta\tau^{(r)}(.) = \tau_L^{(r)}(.) - \tau_0^{(r)}$. The development of the stationarity conditions of $\tilde{w}_L$ w.r.t. $\mathbb{L}_0^{(r)}, \boldsymbol{\tau}_0^{(r)}, f_0^{(r)}$ leads to the following system of equations

$$\begin{cases} \left(\mathbb{L}_L^{(r)} - \mathbb{L}_0^{(r)}\right) : C^{(r)}\left(\boldsymbol{\varepsilon}_0\right) : \left(\mathbb{L}_L^{(r)} - \mathbb{L}_0^{(r)}\right) = C^{(r)}\left(\boldsymbol{\tau}_L^{(r)}\right) \\ \boldsymbol{\tau}_0^{(r)} = \overline{\boldsymbol{\tau}_L}^{(r)} + \left(\mathbb{L}_L^{(r)} - \mathbb{L}_0^{(r)}\right) : \overline{\boldsymbol{\varepsilon}_0}^{(r)} \\ f_0^{(r)} = 0, \end{cases} \tag{70}$$

where the notation $C^{(r)}(\boldsymbol{a})$ for any second-order tensor $\boldsymbol{a}$ is defined by Eq. (10) and where $\boldsymbol{\varepsilon}_0$ corresponds to the strain field within the LCC defined by $w_0^{(r)}$.
It should be noted that both Eqs. $(70)_1$ and $(70)_2$ allow to compute $\mathbb{L}_0^{(r)}$ and $\boldsymbol{\tau}_0^{(r)}$ once the first and second-order moments of $\boldsymbol{\varepsilon}_0$ are known. As recalled in the Appendix D of [1] focused on the case of a $N$-phase thermoelastic composite whose per-phase free-energy $w_0^{(r)}$ is defined by Eq. (67), both these moments are classically obtained by Eq. (D.3) of this Appendix, with explicit analytic expressions in the case of composites with isotropic local stiffness tensors, as for the applications considered hereafter.
We can now derive the effective behavior of the nonlinear composite by making use of Eq. (65) together with (68) such that we have

$$\boldsymbol{\Sigma} = \frac{\partial \tilde{w}_\Delta}{\partial \boldsymbol{E}}(\boldsymbol{E}) \approx \frac{\partial \tilde{w}_L}{\partial \boldsymbol{E}}(\boldsymbol{E}) = \frac{\partial \tilde{w}_0}{\partial \boldsymbol{E}}(\boldsymbol{E}) = \tilde{\mathbb{L}}_0 : \boldsymbol{E} + \tilde{\boldsymbol{\tau}}_0, \tag{71}$$

where the third equality in (71) comes from the stationarity of $\tilde{w}_L$ w.r.t. $\mathbb{L}_0^{(r)}$, $\boldsymbol{\tau}_0^{(r)}$, $f_0^{(r)}$ and the last equality from the expression (D.2) of the effective energy $\tilde{w}_0$ provided in Appendix D of [1]. The tensors $\tilde{\mathbb{L}}_0$ and $\tilde{\boldsymbol{\tau}}_0$ stand for the effective tensor of moduli and the effective polarization of the LCC with local energy $w_0$,

respectively.

Finally, the first and second-order moments of the local strain field of the nonlinear composite are approximated by the ones of the LCC with energy $w_L$ which are themselves (see Lahellec et al. [29]) approximated by the ones of the LCC of energy $w_0$ such that

$$\overline{\boldsymbol{\varepsilon}}^{(r)} \approx \overline{\boldsymbol{\varepsilon}_L}^{(r)} \approx \overline{\boldsymbol{\varepsilon}_0}^{(r)}, \quad \langle \boldsymbol{\varepsilon} \otimes \boldsymbol{\varepsilon} \rangle^{(r)} \approx \langle \boldsymbol{\varepsilon}_L \otimes \boldsymbol{\varepsilon}_L \rangle^{(r)} \approx \langle \boldsymbol{\varepsilon}_0 \otimes \boldsymbol{\varepsilon}_0 \rangle^{(r)}, \tag{72}$$

where $\boldsymbol{\varepsilon}$, $\boldsymbol{\varepsilon}_L$ stand for the strain fields of the nonlinear composite and of the LCC of energy $w_L$, respectively. The same approximations are used to evaluate the first and second-order moments of the stress fields.

*4.3.2. Elastoplastic composites with isotropic phases*

In this work, the behavior of the phases described in Section 4.1 is assumed to be isotropic. For simplicity, the elastic tensors of the LCC with energy $w_0^{(r)}$ are also chosen isotropic such that

$$\mathbb{L}^{(r)} = 3\,k^{(r)}\mathbb{J} + 2\,\mu^{(r)}\mathbb{K}, \quad \mathbb{L}_0^{(r)} = 3\,k_0^{(r)}\mathbb{J} + 2\,\mu_0^{(r)}\mathbb{K}. \tag{73}$$

As shown by Eq. $(61)_2$, the tensor $\boldsymbol{\tau}_L^{(r)}$ is purely deviatoric since $\boldsymbol{\varepsilon}_n^p$ and $\boldsymbol{\nu}_n$ are deviatoric so that $C^{(r)}(\boldsymbol{\tau}_L) :: \mathbb{J} = 0$. Accordingly, from Eq. $(70)_1$ we get

$$\left(k_0^{(r)} - k_L^{(r)}\right)^2 C^{(r)}(\boldsymbol{\varepsilon}_0) :: \mathbb{J} = 0. \tag{74}$$

Since $\boldsymbol{\varepsilon}_0$ has a non constant spherical part in phase $r$ (as it is the case for a Hashin-Shtrikman heterogeneous material), it comes $k_0^{(r)} = k_L^{(r)}$. Moreover, Eq. $(61)_1$

implies that $k_L^{(r)} = k^{(r)}$ so that

$$k^{(r)} = k_L^{(r)} = k_0^{(r)}. \tag{75}$$

Finally, Eq. (75) combined with Eq. $(70)_2$ lead to a purely deviatoric tensor $\boldsymbol{\tau}_0$. Accordingly, the system (61) takes the form

$$\begin{cases} \mathbb{L}_L^{(r)} = 3k_L^{(r)}\mathbb{J} + 2\mu_L^{(r)}\mathbb{K} = 3k^{(r)}\mathbb{J} + 2\mu^{(r)}\left(B^{(r)} - C^{(r)}\right)\mathbb{K} \\ \boldsymbol{\tau}_L^{(r)}(\underline{x}) = -2\mu^{(r)}\left(B^{(r)}\boldsymbol{\varepsilon}_n^p(\underline{x}) + C^{(r)}\boldsymbol{\nu}_n(\underline{x})\right) \\ f_L^{(r)}(\underline{x}) = 2\,\dfrac{\eta_{\varepsilon^p}^{(r)}}{\Delta t}\left(A^{(r)} - C^{(r)}\right)\boldsymbol{\varepsilon}_n^p : \boldsymbol{\varepsilon}_n^p + a_{NL}^{(r)}\left(A^{(r)} + B^{(r)}\right)\boldsymbol{\nu}_n : \boldsymbol{\nu}_n + 2\,a_{NL}^{(r)}\,B^{(r)}\boldsymbol{\varepsilon}_n^p : \boldsymbol{\nu}_n, \end{cases} \tag{76}$$

with

$$A^{(r)} = \frac{2\mu^{(r)}}{2\mu^{(r)} + 2\,\frac{\eta_{\varepsilon^p}^{(r)}}{\Delta t} + a_{NL}^{(r)}}, \quad B^{(r)} = \frac{2\,\eta_{\varepsilon^p}^{(r)}/\Delta t}{2\mu^{(r)} + 2\,\frac{\eta_{\varepsilon^p}^{(r)}}{\Delta t} + a_{NL}^{(r)}}, \quad C^{(r)} = A^{(r)} + B^{(r)} - 1. \tag{77}$$

Likewise, Eqs. (51) and (52) can be recast as

$$\boldsymbol{\varepsilon}^p = A^{(r)}\boldsymbol{\varepsilon}_d + B^{(r)}\boldsymbol{\varepsilon}_n^p + C^{(r)}\boldsymbol{\nu}_n, \tag{78}$$

$$\boldsymbol{\nu} = P^{(r)}\boldsymbol{\varepsilon}_d + Q^{(r)}\boldsymbol{\varepsilon}_n^p + R^{(r)}\boldsymbol{\nu}_n, \tag{79}$$

with

$$P^{(r)} = -\frac{a_{NL}^{(r)}\Delta t}{2\,\eta_\nu^{(r)}}A^{(r)}, \quad Q^{(r)} = -\frac{a_{NL}^{(r)}\Delta t}{2\,\eta_\nu^{(r)}}B^{(r)}, \quad R^{(r)} = \frac{a_{NL}^{(r)}}{a^{(r)}}\left(A^{(r)} + B^{(r)}\right) - C^{(r)}, \tag{80}$$

where $\boldsymbol{\varepsilon}_d$ denotes the deviatoric part of $\boldsymbol{\varepsilon}$. In order to evaluate $\mathbb{L}_L^{(r)}$ and $\boldsymbol{\tau}_L^{(r)}$ (in fact only $\overline{\boldsymbol{\tau}}_L^{(r)}$ is required), expressions $(76)_{1,2}$ show that we have to determine the

viscosities $\eta_{\varepsilon^p}^{(r)}$ and $\eta_{\nu}^{(r)}$ characterized by Eqs. $(49)_2$ and (58). For that, we need to compute $\overline{\overline{\dot{\varepsilon}^p}}^{(r)}$ and $\overline{\overline{\dot{\nu}}}^{(r)}$ (cf. Eqs. $(49)_2$ and (58)) since all the other quantities are known. The calculation of both these second-order moments is reported in AppendixB since it leads to cumbersome expressions. However, it should be noted that the determination of $\overline{\overline{\dot{\varepsilon}^p}}^{(r)}$ and $\overline{\overline{\dot{\nu}}}^{(r)}$ in AppendixB is obtained by making use of the essential following assumption

**Assumption 4.**

$$C^{(r)}\left(\dot{\boldsymbol{\nu}}\right) :: \mathbb{K} = \mathbf{0} \Leftrightarrow \overline{\dot{\nu}}_{eq}^{(r)} = \overline{\overline{\dot{\nu}}}^{(r)} \quad \textit{with} \quad \overline{\dot{\nu}}_{eq}^{(r)} = \sqrt{\frac{2}{3}\,\overline{\dot{\boldsymbol{\nu}}}^{(r)} : \overline{\dot{\boldsymbol{\nu}}}^{(r)}}, \tag{81}$$

postulated in order to close the nonlinear system to be solved.

**Remark 1.** *Assumption* (4) *amounts to say that the field $\dot{\boldsymbol{\nu}}$ is homogeneous per phase, or equivalently, by means of Eq.* $(54)_2$*, that the back stress $\boldsymbol{X}$ is also homogeneous per phase. Furthermore, recalling that $X$ is defined by* $(34)_2$*, it comes that the kinematic hardening variable $\boldsymbol{\beta} = \boldsymbol{\varepsilon^p} + \boldsymbol{\nu}$ is homogeneous per phase too. This fact would be consistent with the mean-field type approximation* (40) *which would then be an exact consequence of assumption* (4) *and no longer an approximation.*

*Of course, assumption* (4) *which amounts to the homogeneity of the back stress within the phases, thus neglecting its intraphase fluctuations, is an ad-hoc assumption and not an optimal choice, for instance which would have been derived by means of some stationarity conditions to be defined. However, it leads to a DIV model which provides accurate estimates of both the effective behavior as well as the statistics of the local fields, even for multi-cyclic loadings, as it will be shown in Section 5. Such an accurate description of the real behavior of elasto-plastic*

*composites, even for multi-cyclic loadings, shows that the ad-hoc assumption* (4)*, even not optimal, is therefore relevant.*

*4.4. Application to an elasto-plastic matrix reinforced by linear elastic particles*

The DIV formulation is now applied to the case of two-phase composites made of an elasto-plastic matrix with both nonlinear kinematic and isotropic hardening reinforced by linear elastic particles randomly and isotropically distributed inside the matrix. In this case, there is only one nonlinear phase for such two-phase isotropic materials. The effective behavior of the LCC with free energy $w_0$ as well as the statistics of its local fields can be evaluated by the Hashin-Shtrikman lower bound which is known to be appropriate for such type of microstructure for moderate volume fractions. In the sequel, subscripts (1) and (2) stand for the inclusion and matrix phase, respectively.

The average of $\boldsymbol{\varepsilon}_0$ over each phase reads as

$$\overline{\boldsymbol{\varepsilon}_0}^{(1)} = \mathbb{A}_0^{(1)} : \boldsymbol{E} + \boldsymbol{a}_0^{(1)}, \quad \overline{\boldsymbol{\varepsilon}_0}^{(2)} = \frac{1}{c^{(2)}} \left( \boldsymbol{E} - c^{(1)} \overline{\boldsymbol{\varepsilon}_0}^{(1)} \right), \tag{82}$$

with

$$\mathbb{A}_0^{(1)} = \left[ \mathbb{I} + c^{(2)} \mathbb{P}_0^{(2)} : \left( \mathbb{L}_0^{(1)} - \mathbb{L}_0^{(2)} \right) \right]^{-1} \quad \text{and} \quad \boldsymbol{a}_0^{(1)} = c^{(2)} \mathbb{A}_0^{(1)} : \mathbb{P}_0^{(2)} : \left( \boldsymbol{\tau}_0^{(2)} - \boldsymbol{\tau}_0^{(1)} \right).$$

Tensor $\mathbb{P}_0^{(2)}$ corresponds to the classical Hill's tensor associated with the matrix phase of the homogeneous LCC for an isotropic distribution of inclusions. Substituting in these relations the uniform polarisations $\boldsymbol{\tau}_0^{(r)}$ by their expressions given

in $(70)_2$, one obtains the following relation for the average strain in the inclusions

$$\begin{aligned}\overline{\boldsymbol{\varepsilon}_0}^{(1)} = &\left\{\mathbb{I}+\mathbb{P}_0^{(2)} : \left[\left(\mathbb{L}_L^{(1)}-\mathbb{L}_0^{(2)}\right) - c^{(1)}\left(\mathbb{L}_L^{(1)}-\mathbb{L}_L^{(2)}\right)\right]\right\}^{-1} : \\ &\left\{\left[\mathbb{I}+\mathbb{P}_0^{(2)} : \left(\mathbb{L}_L^{(2)}-\mathbb{L}_0^{(2)}\right)\right] : \boldsymbol{E} - c^{(2)}\mathbb{P}_0^{(2)} : \left(\overline{\boldsymbol{\tau}_L}^{(1)} - \overline{\boldsymbol{\tau}_L}^{(2)}\right)\right\}.\end{aligned} \tag{83}$$

The use of the Hashin-Shtrikman bound to evaluate the strain field in the LCC implies that the latter is uniform inside the inclusions, i.e. $C^{(1)}(\boldsymbol{\varepsilon}_0) = \mathbf{0}$. Eq. $(70)_1$ requires then that $C^{(1)}(\boldsymbol{\tau}_L^{(1)}) = 0$, which is actually true from Eq. $(61)_2$: the fields $\boldsymbol{\varepsilon}_n^p$ and $\boldsymbol{\nu}_n$ are naturally null in the elastic inclusion phase. In such a case $(70)_1$ does not provide any prescription to determine $\mathbb{L}_0^{(1)}$ and it is natural to chose, as in Lahellec et al. [29]

$$\mathbb{L}_0^{(1)} = \mathbb{L}_L^{(1)}, \tag{84}$$

Finally Eq. $(70)_2$ implies

$$\boldsymbol{\tau}_0^{(1)} = \overline{\boldsymbol{\tau}_L}^{(1)} = 0. \tag{85}$$

*4.4.1. Summary of the nonlinear system of equations*

In this Section, we summarize the equations that the DIV formulation should satisfy. First, we have to recall Eq. (75) which is satisfied for both phases. Within the elastic inclusions, we have $\overline{\overline{\dot{\varepsilon}^p}}^{(1)} = 0$ and $\overline{\overline{\dot{\nu}}}^{(1)} = 0$ such that $\eta_{\varepsilon^p}^{(1)}$ and $\eta_\nu^{(1)}$ tend to infinity because of Eqs. (49) and $(55)_2$. Then, reporting Eq. (53) into Eq. $(76)_1$ leads to equality $\mu^{(1)} = \mu_L^{(1)}$. Making use of Eqs. (84) and (85), we finally obtain the behavior within the inclusion phase of the LCCs defined by $w_L$ and $w_0$ which reads as follows

$$k^{(1)} = k_L^{(1)} = k_0^{(1)}, \quad \mu^{(1)} = \mu_L^{(1)} = \mu_0^{(1)}, \quad \boldsymbol{\tau}_0^{(1)} = \overline{\boldsymbol{\tau}_L}^{(1)} = 0. \tag{86}$$

For the matrix phase, the LCCs $w_0$ and $w_L$ are characterized by the properties $\mu_0^{(2)}$, $\boldsymbol{\tau}_0^{(2)}$, $\mu_L^{(2)}$, $\boldsymbol{\tau}_L^{(2)}$ which are obtained as follows. The shear modulus $\mu_L^{(2)}$ and polarization $\boldsymbol{\tau}_L^{(2)}$ are given by Eqs. $(76)_1$ and $(76)_2$, respectively. The expression of the polarization $\boldsymbol{\tau}_0^{(2)}$ is obtained by applying Eq. $(70)_2$ to isotropic phases, which then reads

$$\boldsymbol{\tau}_0^{(2)} = \overline{\boldsymbol{\tau}_L}^{(2)} + 2\left(\mu_L^{(2)} - \mu_0^{(2)}\right)\overline{\boldsymbol{\varepsilon}_{0,d}}^{(2)}. \tag{87}$$

Similarly, applying $(70)_1$ to isotropic LCCs leads to

$$\mu_0^{(2)} = \mu_L^{(2)} \pm \frac{1}{2}\sqrt{\frac{\langle \boldsymbol{\tau}_L : \boldsymbol{\tau}_L \rangle^{(2)} - \overline{\boldsymbol{\tau}_L}^{(2)} : \overline{\boldsymbol{\tau}_L}^{(2)}}{\langle \boldsymbol{\varepsilon}_{0,d} : \boldsymbol{\varepsilon}_{0,d} \rangle^{(2)} - \overline{\boldsymbol{\varepsilon}_{0,d}}^{(2)} : \overline{\boldsymbol{\varepsilon}_{0,d}}^{(2)}}}. \tag{88}$$

It should be noted that once the viscosities $\eta_{\varepsilon^p}^{(2)}$ and $\eta_\nu^{(2)}$ - or equivalently $\overline{\overline{\dot{\varepsilon}^p}}^{(2)}$ and $\overline{\overline{\dot{\nu}}}^{(2)}$ (cf. $(49)_2$ and (58)) - are known, the numerator in the square root of Eq. (88) is also known since $\boldsymbol{\tau}_L$ depends linearly on $\boldsymbol{\varepsilon}_n^p$ and $\boldsymbol{\nu}_n$ (see Eq. $(76)_2$) whose first and second-order moments are determined from the former step. For the denominator, the first-order moment $\overline{\boldsymbol{\varepsilon}_{0,d}}^{(2)}$ and the second-order moment $\langle \boldsymbol{\varepsilon}_{0,d} : \boldsymbol{\varepsilon}_{0,d} \rangle^{(2)}$ are obtained from Eqs. (82), (83) and (B.5). For isotropic composites, these moments depend on the properties $\mu_0^{(2)}$ and $\boldsymbol{\tau}_0^{(2)}$ which characterize the matrix behavior of the LCC of energy $w_0$. Therefore, the nonlinear problem to be solved is made of the four Eqs. $(49)_1$, $(49)_2$, (87) and (88) with four unknowns $\eta_{\varepsilon^p}^{(2)}$, $\eta_\nu^{(2)}$, $\boldsymbol{\tau}_0^{(2)}$ and $\mu_0^{(2)}$.

In addition, as shown by Eqs. $(49)_2$ and (58), the determination of $\eta_{\varepsilon^p}^{(2)}$ and $\eta_\nu^{(2)}$ amounts to compute $\overline{\overline{\dot{\varepsilon}^p}}^{(2)}$ and $\overline{\overline{\dot{\nu}}}^{(2)}$. To this end, we make use of Eqs. (B.1) and (B.2) which themselves require to evaluate the second-order moments $\langle \boldsymbol{\varepsilon}_d : \boldsymbol{\varepsilon}_n^p \rangle^{(2)}$

and $\langle \boldsymbol{\varepsilon}_d : \boldsymbol{\nu}_n \rangle^{(2)}$. These moments can be derived from Eqs. (B.4), (B.9) and (B.7) and from the computation of $\overline{\boldsymbol{\varepsilon}_{0,d}}^{(2)}$ and $\langle \boldsymbol{\varepsilon}_{0,d} : \boldsymbol{\varepsilon}_{0,d} \rangle^{(2)}$ which are given by Eqs. (82), (83) and (B.5).

Lastly, by making use of the expression of $\mathbb{P}_0^{(2)}$ for an isotropic composite together with Eqs. (82) and (83), it is observed that $\overline{\boldsymbol{\varepsilon}_{0,d}}^{(2)}$ does no more depend on $\boldsymbol{\tau}_0^{(2)}$ but only on the three independent parameters $\mu_0^{(2)}$, $\eta_{\varepsilon^p}^{(2)}$ and $\eta_\nu^{(2)}$. Keeping in mind this dependence together with associating Eq. (87) with the definitions (76) of $\mu_L^{(2)}$ and $\boldsymbol{\tau}_L^{(2)}$, it is shown that the polarization $\boldsymbol{\tau}_0^{(2)}$ also depends only on the three parameters $\mu_0^{(2)}$, $\eta_{\varepsilon^p}^{(2)}$ and $\eta_\nu^{(2)}$.

As a consequence, the initial nonlinear problem to be solved and defined by Eqs. $(49)_2$, (58), (87) and (88) now reduces to a nonlinear system of three scalar equations $(49)_2$, (58) and (88) with three unknowns $\eta_{\varepsilon^p}^{(2)}$, $\eta_\nu^{(2)}$ and $\mu_0^{(2)}$ which can be rewritten as follows

$$\begin{cases} F_1\left(\mu_0^{(2)}, \eta^{(2)}\right) \equiv \left(\mu_0^{(2)} - \mu_L^{(2)}\right)^2 - \dfrac{1}{4} \dfrac{\langle \boldsymbol{\tau}_L : \boldsymbol{\tau}_L \rangle^{(2)} - \overline{\boldsymbol{\tau}_L}^{(2)} : \overline{\boldsymbol{\tau}_L}^{(2)}}{\langle \boldsymbol{\varepsilon}_{0,d} : \boldsymbol{\varepsilon}_{0,d} \rangle^{(2)} - \overline{\boldsymbol{\varepsilon}_{0,d}}^{(2)} : \overline{\boldsymbol{\varepsilon}_{0,d}}^{(2)}} = 0 \\ F_2\left(\mu_0^{(2)}, \eta^{(2)}\right) \equiv \eta_{\varepsilon^p}^{(2)} - \dfrac{\sigma_y^{(2)} + R^{(2)}\left(p_n^{(2)} + \Delta t \, \overline{\dot{\varepsilon}^p}^{(2)}\right)}{3\,\overline{\dot{\varepsilon}^p}^{(2)}} = 0 \\ F_3\left(\mu_0^{(2)}, \eta^{(2)}\right) \equiv \eta_\nu^{(2)} - \dfrac{a^{(2)}}{2\,\gamma^{(2)}\,\overline{\dot{\varepsilon}^p}^{(2)}} = 0. \end{cases} \tag{89}$$

This system needs to be solved at each elastoplastic loading step with an appropriate solver. Details are provided in Section 4.5. Once the solution is reached, all quantities under consideration can be computed at the end of this loading step and one can proceed to the next time increment.

At this stage it is worth noting that many of the above introduced quantities depend on the full fields of internal variables, which might all be heterogeneous, with the exception of $\boldsymbol{\beta} = \boldsymbol{\varepsilon}^p + \boldsymbol{\nu}$ which is homogeneous as discussed in remark

1. The computation of these quantities requires however only a limited number of tensorial or scalar variables that describe these fields. More precisely, it turns out that the following $5$ variables are sufficient: the first order moments $\overline{\boldsymbol{\varepsilon}_n^p}^{(2)}$ and $\overline{\boldsymbol{\nu}_n}^{(2)}$, the second order moments $\overline{\overline{\varepsilon_n^p}}^{(2)}$ and $\overline{\overline{\nu_n}}^{(2)}$ and the scalar $p_n^{(2)}$.

*4.4.2. Elastic regime*

The elastic regime is dealt with in a way similar to that used in [1]. We focus here on the specific developments associated with the nonlinear kinematic hardening. As seen in Section 4.2, the surface of plasticity is reached when Eq. (59) is satisfied in the matrix phase. Accordingly, to test if the matrix is in the elastic domain, one needs to check that the second-order moment $\overline{\overline{\sigma_d - X}}^{(2)}$ satisfies the following inequality

$$\overline{\overline{\sigma_d - X}}^{(2)} < \sigma_y^{(2)} + R^{(2)}(p^{(2)}), \tag{90}$$

which can be interpreted as an effective yield criterion of the matrix. For that, $\overline{\overline{\sigma_d - X}}^{(2)}$ should be computed for each time increment to specify whether it is an elastic or a plastic one. Starting from the definition of $\overline{\overline{\sigma_d - X}}^{(2)}$, we have

$$\overline{\overline{\sigma_d - X}}^{(2)} = \sqrt{\left(\overline{\overline{\sigma_d}}^{(2)}\right)^2 + \left(\overline{\overline{X}}^{(2)}\right)^2 - 3\,\left\langle \boldsymbol{\sigma}_d : \boldsymbol{X} \right\rangle^{(2)}}, \tag{91}$$

where $\overline{\overline{\sigma_d}}^{(2)}$ is determined by (B.7). In the case of an elastic increment, Eq. $(34)_2$ together with $\boldsymbol{\varepsilon}^p = \boldsymbol{\varepsilon}_n^p$ and $\boldsymbol{\nu} = \boldsymbol{\nu}_n$ leads to $\overline{\overline{X}}^{(2)} = \frac{3}{2} a^{(2)} \left(\overline{\overline{\varepsilon_n^p + \nu_n}}^{(2)}\right)$.
In order to determine the average product $\left\langle \boldsymbol{\sigma}_d : \boldsymbol{X} \right\rangle^{(2)}$, it is useful to recall remark 1 which indicates that one of the consequences of assumption (81) is that the field $\boldsymbol{X}$ is homogeneous in the matrix phase during a plastic increment, and will remain so in an elastic one, so that $\left\langle \boldsymbol{\sigma}_d : \boldsymbol{X} \right\rangle^{(2)} = \overline{\boldsymbol{\sigma}_d}^{(2)} : \overline{\boldsymbol{X}}^{(2)}$ where $\overline{\boldsymbol{X}}^{(2)} =$

$a^{(2)}\left(\overline{\boldsymbol{\varepsilon}_n^p}^{(2)}+\overline{\boldsymbol{\nu}_n}^{(2)}\right)$ is known for the former step and $\overline{\boldsymbol{\sigma}_d}^{(2)}$ is evaluated by $\overline{\boldsymbol{\sigma}_d}^{(2)} \approx \overline{\boldsymbol{\sigma}_{0,d}}^{(2)} = 2\,\mu_0^{(2)}\overline{\boldsymbol{\varepsilon}_{\mathbf{0},\boldsymbol{d}}}^{(2)} + \boldsymbol{\tau}_0^{(2)}$. Accordingly, all the quantities on which relies the inequality (90) are determined, thus allowing to check if the composite is in the elastic or plastic regime.

*4.5. Numerical implementation of the model and computational issues*

In the present study, we make use of the same algorithm as the one presented by Lucchetta et al. in [1] for two-phase elastoplastic composites with linear kinematic and isotropic hardening. Indeed, the problem to be solved here, which corresponds to the nonlinear system (89), has exactly the same structure than the one handled by Lucchetta et al. (see Eq. (82) in [1]). The only difference is that there is now one additional unknown $\eta_\nu^{(2)}$ and nonlinear equation $F_3 = 0$, with $F_3$ defined by $(89)_3$, both induced by the introduction of the kinematic hardening variable $\beta$. The reader interested by the algorithm of the DIV formulation is therefore referred to [1] where a detailed description is provided.

Let us however stress that the nonlinear system (89) has at least two roots since Eq. $(89)_1$ can be rewritten as

$$F_1^{\pm}\left(\mu_0^{(2)},\eta_{\varepsilon^p}^{(2)}\right) \equiv \mu_0^{(2)} - \mu_L^{(2)} \pm \frac{1}{2}\sqrt{\frac{\left\langle \boldsymbol{\tau}_L : \boldsymbol{\tau}_L \right\rangle^{(2)} - \overline{\boldsymbol{\tau}_L}^{(2)} : \overline{\boldsymbol{\tau}_L}^{(2)}}{\left\langle \boldsymbol{\varepsilon}_0^d : \boldsymbol{\varepsilon}_0^d \right\rangle^{(2)} - \overline{\boldsymbol{\varepsilon}_0^d}^{(2)} : \overline{\boldsymbol{\varepsilon}_0^d}^{(2)}}} = 0, \qquad (92)$$

where $F_1^+$ and $F_1^-$ respectively denote the function $F_1^{\pm}$ associated with the signs $+$ and $-$ before the square root. In practice, it is numerically observed that the function $F_1$ defined by $(89)_1$ has several roots w.r.t the variable $\mu_0^{(2)}$ at fixed $\eta_{\varepsilon^p}^{(2)}$ and $\eta_\nu^{(2)}$: two as expected for composites with incompressible phases but even four for compressible composites. A numerical method to select the appropriate

solution of system (89) has been proposed by Lucchetta et al. in [1]. For the sake of conciseness, this method is not presented here and the reader interested by this non uniqueness issue is referred to [1]. Mention can also be made of the very recent works of Cotelo et al. [31] and Idiart et al. [32], [33] addressing this difficult issue. The main results obtained by using the method proposed by Lucchetta et al. [1] are the followings: when applied to elastoplastic two-phase composites with linear kinematic hardening, it is observed that this method works well for incompressible composites. However, for compressible composites, due to the occurrence of four roots and the presence of singularities, this method fails to determine the appropriate root at some scarce points. In the case of elastoplastic two-phase composites with nonlinear kinematic hardening, the same numerical observations can be made even if sometimes the convergence towards the appropriate root is less efficient for the nonlinear kinematic hardening case than for the linear one. Accordingly, in order to avoid the above-mentioned numerical difficulties encountered for compressible phases, we only consider incompressible composites in all the simulations which will be carried out in the sequel by means of the DIV formulation.

## 5. Assessment of the DIV model

This section aims to compare the results obtained by the DIV formulation associated with the modified Chaboche model to Finite Element (FE) simulations that we carried out through the software Cast3M. These simulations have been performed on two-phase periodic composites made of spherical elastic particles embedded in a perfect cubic lattice in an elastoplastic matrix described by the Armstrong-Frederick model. The DIV approach is applied to elastoplastic incom-

pressible composites made of isotropic elastic inclusions, randomly and isotropically distributed in an elastoplastic matrix. Use is made of the lower Hashin-Shtrikman bound to homogenize the LCC with energy $w_0$. Corresponding relations can for instance be found in Appendix D of [1]. The matrix exhibits either nonlinear kinematic hardening or combined isotropic and nonlinear kinematic hardening.

It should be noted that the comparisons performed between the DIV formulation and the FE solution present a bias since they do not address the same microstructure, e.g. see [34]. Indeed, the DIV formulation addresses reinforced composites made of inclusions, randomly and isotropically distributed in a matrix while the FE simulations address composites with a periodic cubic spatial distribution of spherical particles. Due to its cubic symmetry, such a composite is anisotropic and its response depends on the direction of loading unlike the isotropic DIV formulation. As shown by Majewski et al. [35] for elastoplastic reinforced composites with isotropic hardening and such cubic microstructures, the dependence of the macroscopic response on the direction of loading is significant for a volume fraction of $20\%$ and above but is negligible for a low volume fraction of $10\%$. The comparisons presented in this section are performed for a volume fraction of $17\%$ for which this bias might be present but is expected to be limited. Such a bias should be kept in mind when interpreting the results of the comparisons. For improved comparisons, additional FE simulations based on multi-inclusions unit cells and elasto-plastic phases with nonlinear kinematic hardening would be required. Such simulations, not available yet in the literature to our best knowledge, would be very time consuming, especially for cycling loading conditions as considered later in this section, and are left to a future work.

The applied loading consists of a macroscopic strain $E(t)$ which is an isochoric extension $E_{33}(t)$ along the axial direction:

$$\boldsymbol{E}(t) = E_{33}(t)\left(-\frac{1}{2}(\boldsymbol{e}_1 \otimes \boldsymbol{e}_1 + \boldsymbol{e}_2 \otimes \boldsymbol{e}_2) + \boldsymbol{e}_3 \otimes \boldsymbol{e}_3\right). \tag{93}$$

In association with (93), two types of loading histories, presented in Fig.1, are considered. The first one corresponds to a cyclic radial extension and the second one to a positive cyclic radial extension.

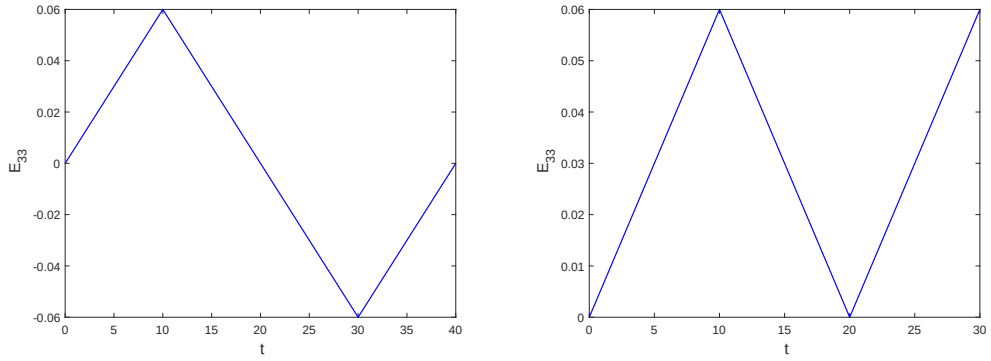


(a) (b)

Figure 1: Loading histories: $E_{33}(t)$ macroscopic axial strain, (a) program 1: cyclic radial extension, (b) program 2: positive cyclic radial extension.

In order to quantify the influence of the time step discretization on the DIV predictions, simulations have been carried out for different values of the time step $\Delta t$ on the same composite material, with a matrix exhibiting a purely nonlinear kinematic hardening. The material parameters are given in (94). It has been found that, for $\Delta t \leq 0.1s$, all the simulations leads to identical results such that the time step is fixed to $\Delta t = 0.1s$ for all the simulations carried out in the sequel.

### *5.1. Application of the DIV approach to reinforced composites exhibiting nonlinear kinematic hardening*

#### *5.1.1. Matrix with nonlinear kinematic hardening*

In this section we consider incompressible elastically reinforced two-phase materials having an elastoplastic matrix with nonlinear kinematic hardening. The material parameters are

$$\begin{aligned} &\text{Inclusion :} \quad c^{(1)} = 0.17, \;\; \mu^{(1)} = 6\,\text{GPa}, \;\; k^{(1)} = 3 \times 10^7\,\text{GPa} \\ &\text{Matrice :} \quad \mu^{(2)} = 3\,\text{GPa}, \;\; k^{(2)} = 1.5 \times 10^7\,\text{GPa}, \;\; \sigma_y^{(2)} = 100\,\text{MPa} \\ &\qquad\qquad a^{(2)} = 100\,\text{MPa}, \;\; \gamma^{(2)} = 70. \end{aligned} \tag{94}$$

The results are reported in Fig. 2. First, it is observed that the DIV model provides accurate predictions of both the macroscopic stress and the average stress in the matrix even though both these stresses are slightly over- or under-estimated, respectively. Moreover, the model reproduces the Bauschinger effect observed on the macroscopic response. However, although the trends of the FE simulations for the average axial stress in the inclusion and the stress fluctuations within the matrix are reproduced, the model significantly overestimates their amplitudes. One notices a small non physical jump for the stress fluctuations within the matrix. This jump comes from the convergence of the algorithm towards an unappropriate solution since, as shown in Section 4.5, the solution of the nonlinear system of equations is not unique. Unlike the linear kinematic hardening case where we solve the convergence problem thanks to numerical constraints (see [1]), in the case of nonlinear kinematic hardening, we did not succeed in fully solving this problem. Black dots in Figure 2 refers to loading times associated with singular points of the stress fluctuations. More particularly, the second, fourth and sev-

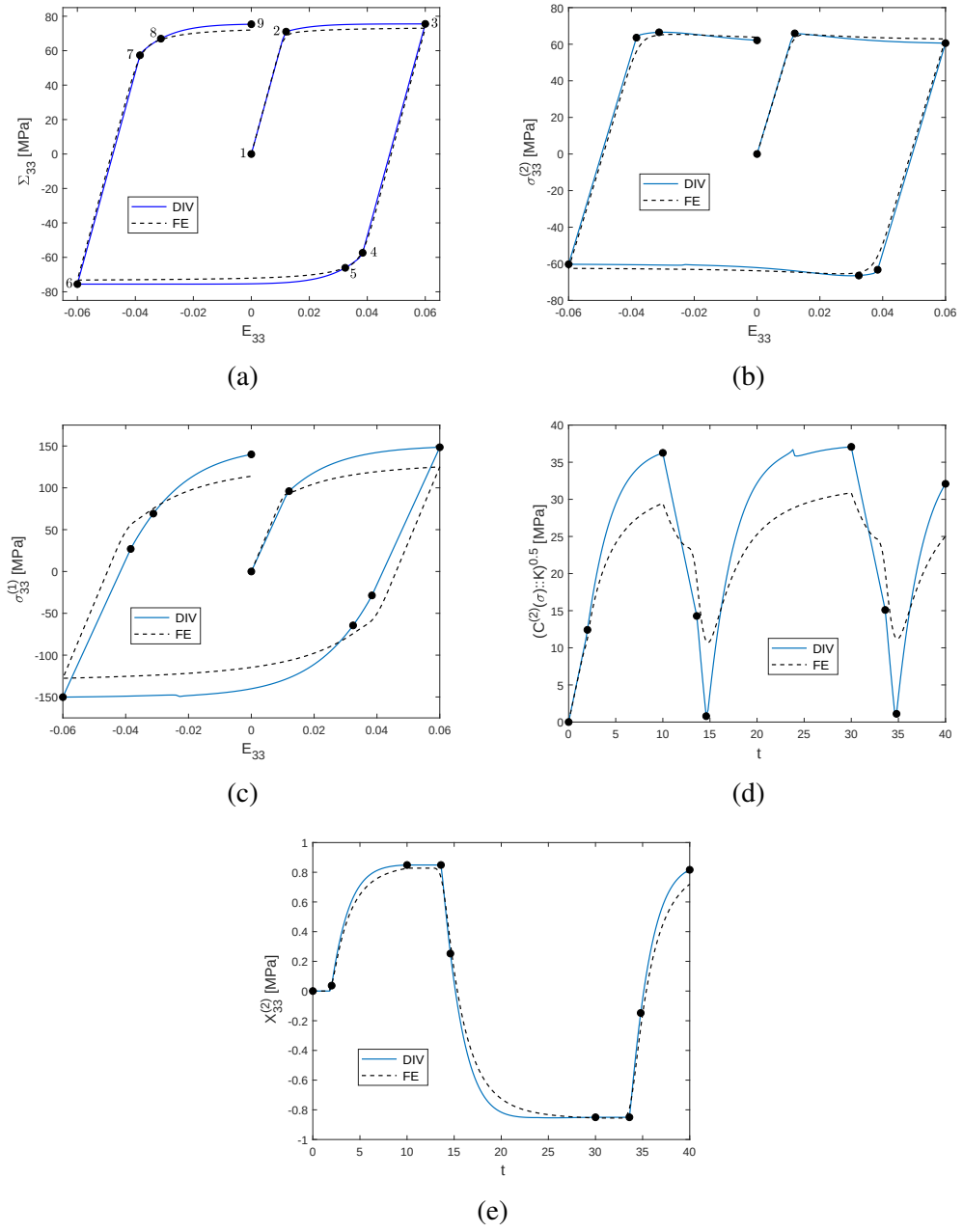


Figure 2: Elastically reinforced composite under cyclic loading (program 1, Fig.1a). Elastoplastic matrix with nonlinear kinematic hardening. $c^{(1)} = 0.17$. Comparison between the DIV formulation and the FE simulations. (a) Macroscopic axial stress, (b) Average axial stress in the matrix, (c) Average axial stress in the inclusion, (d) Stress fluctuations in the matrix, (e) Matrix average of the axial back-stress.

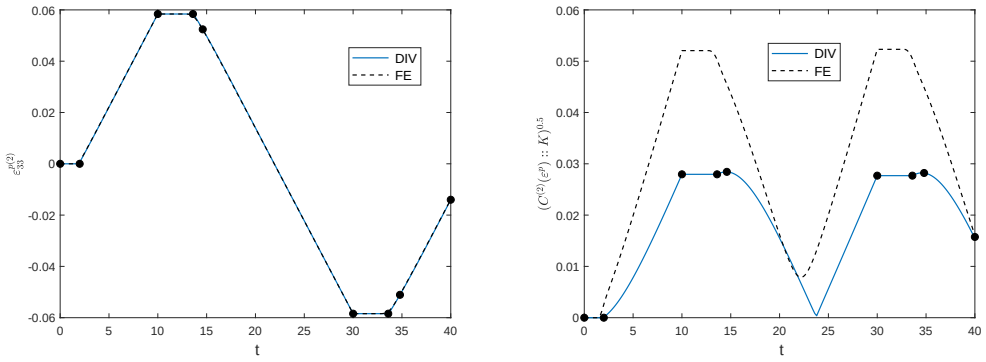


(a) (b)

Figure 3: Elastically reinforced composite under cyclic loading (program 1, Fig.1a). Elastoplastic matrix with nonlinear kinematic hardening. $c^{(1)} = 0.17$. Comparison between the DIV formulation and the FE simulations. (a) Average axial plastic strain, (b) Plastic strain fluctuations in the matrix.

enth points represent the time for which we observe a break in the slope of the stress fluctuations. It is seen in Figures 2a and 2b that these points correspond to the times for which the composite, and also the matrix, go from the elastic to the plastic regime. The fifth and eighth points represent the times for which the stress fluctuations are zero. According to Figure 2a, the discontinuity of the slope of the curve giving the stress fluctuations in Figure 2d at the fourth and seventh points occurs at the transition from the elastic to the plastic regimes. In particular, it is observed in Figure 2b that the times associated with a zero value of the stress fluctuations (points fifth and eighth) correspond to the local extremum of the average stress in the matrix. Moreover, when the stress fluctuations go to zero it is also observed that the average stress in the matrix and in the inclusions and the macroscopic axial stress are almost equal. Indeed before that point, the DIV predicts a stress in the matrix larger than in the inclusions, likely because of the predominance of the back-stress, while after that point the inclusions carry a larger stress

than the matrix, as during the first plastic regime after loading from the natural state, between points 2 to 3. Indeed, it seems that points 5 and 8 are associated with perfectly uniform stress states in the composite material, at least according to the mean-field DIV formulation. In the more refined FE model, the local stress field is never fully uniform, but its fluctuations go anyway to a minimum at a loading stage very close to the one where the fluctuations are zero according to the DIV estimate.

Eventually, it is observed in Fig. 2e that the evolution of the mean value over the matrix of the axial back-stress is well captured by the model even though it slightly overestimates the FE simulations. It is also noted that the evolution of the matrix average of the axial back-stress is nonlinear when plastic flow occurs, thus showing that the proposed DIV model is able to capture the nonlinearity induced by the kinematic hardening. Lastly, note that the evolution of the mean value over the matrix of the kinematic hardening variable $\beta = \varepsilon^p + \nu$ is also provided by Figure 2e since $X = a^{(2)}\beta$. As mentioned in remark 1, its fluctuations in the matrix phase are zero as a consequence of assumption (81).

For the same composite, we also report in Figures 3a and 3b the evolutions of the matrix average of the plastic strain and of its fluctuations, respectively. Regarding the matrix average of the axial plastic strain, a very good agreement is observed between the DIV model and the FE simulations while for the plastic strain fluctuations in the matrix, the DIV model qualitatively captures the trends of the FE predictions but fails to reproduce its evolution quantitatively since it significantly underestimates the heterogeneity of the plastic strain field predicted by the FE simulations. This is not that surprising, as a mean-field approach based on limited ways to describe a heterogeneous local field may naturally be less efficient than

a full-field simulation making use of a very large number of degrees of freedom. At least Figure 3b shows that the DIV formulation considers local heterogeneous plastic strain field, unlike many more classical mean-field theories which simply manipulate their per-phase average values, and often assume, implicitly or explicitly, that they are homogeneous in the phases. Note also that the prediction of the average plastic strain in the matrix, is actually not a big challenge in the present case of a single nonlinear phase and elastic strains small w.r.t. plastic ones. In such a case, the elastic strains in both the inclusions and the matrix are very small w.r.t. the plastic strains in the matrix, so that the average condition $\langle \boldsymbol{\varepsilon} \rangle = \boldsymbol{E}$, reads $\langle \boldsymbol{\varepsilon} \rangle = c^{(1)} \langle \boldsymbol{\varepsilon} \rangle^{(1)} + c^{(2)} \langle \boldsymbol{\varepsilon}^e + \boldsymbol{\varepsilon}^p \rangle^{(2)} \approx c^{(2)} \langle \boldsymbol{\varepsilon}^p \rangle^{(2)}$ so that, except when plastic strains are small, one has $\langle \boldsymbol{\varepsilon}^p \rangle^{(2)} = \frac{1}{c^{(2)}} \boldsymbol{E}$. This explains the rather perfect agreement between FE simulations and DIV models in Figure 3a. But Figure 3b clearly shows that the DIV formulation is able to go much further than such simple considerations.

*5.1.2. Matrix with combined isotropic and nonlinear kinematic hardening*

We now consider an elastoplastic matrix with combined isotropic and nonlinear kinematic hardening. The isotropic hardening rule is expressed by

$$R^{(2)}(p) = \left(R_{max} - \sigma_y^{(2)}\right) \left(1 - e^{-\beta\, p}\right). \tag{95}$$

The material parameters are given by Eq. (94) for the elastic properties of the phases and by the following parameters for the nonlinear kinematic hardening

$$a^{(2)} = 5\,\text{GPa} \quad \text{and} \quad \gamma^{(2)} = 40, \tag{96}$$

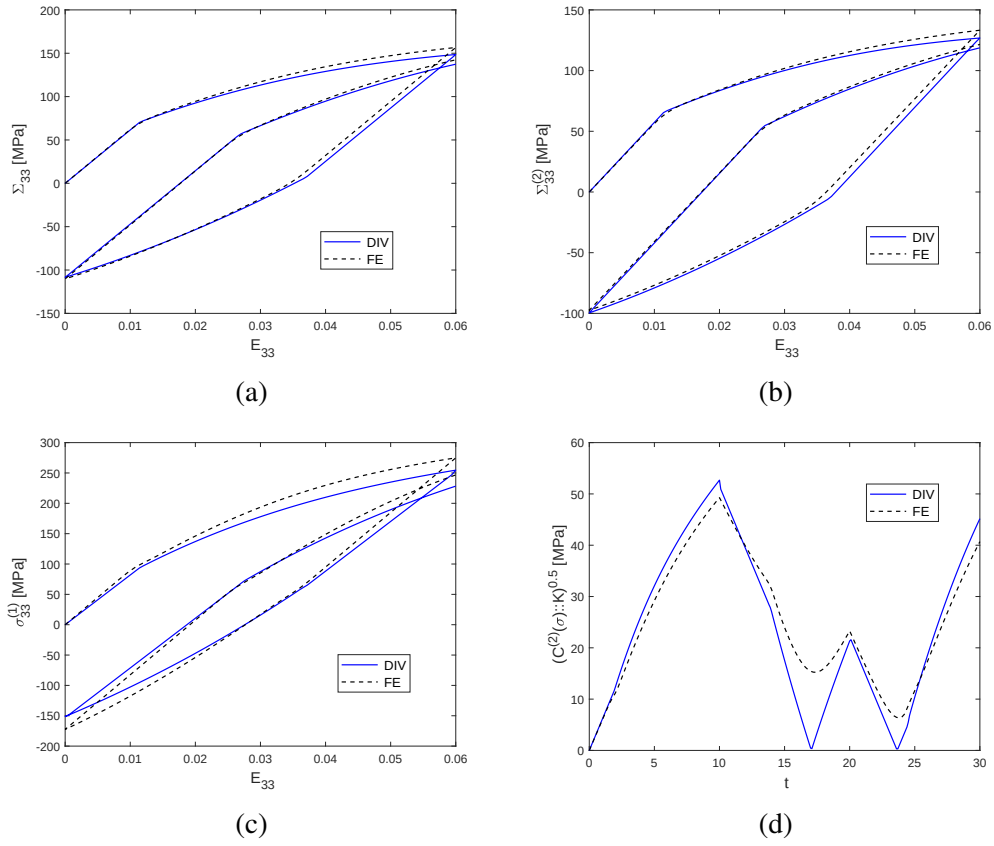


Figure 4: Elastically reinforced composite under cyclic loading (program 2, Fig.1b). Case of an elastoplastic matrix with combined isotropic and nonlinear kinematic hardening. $c^{(1)} = 0.17$. Comparison between the DIV formulation and the FE simulations. (a) Macroscopic axial stress, (b) Average axial stress in the matrix, (c) Average axial stress in the inclusion, (d) Stress fluctuations in the matrix

and the isotropic hardening

$$R_{max} = 1\,\text{GPA} \quad \text{and} \quad \beta = 0.26. \tag{97}$$

The composite is now submitted to a macroscopic cyclic extension corresponding to program 2 (see Fig. 1b). Fig. 4 depicts the evolutions of the axial macroscopic

stress, the average axial stress in the phases as well as the stress fluctuations in the matrix given by the DIV formulation and the FE simulations. It is observed for the macroscopic response and the local responses in the matrix and inclusions a good agreement between the DIV predictions and the FE simulations even if the amplitudes in these latter are slightly underestimated by the model. We also note that the Bauschinger effect is well captured. However, although the DIV model reproduces qualitatively the FE simulations for the average stress in the inclusions, its agreement with the FE computations is less accurate than the one observed for the matrix and macroscopic responses. Lastly, we observe that the DIV formulation reproduces qualitatively and quantitatively the stress fluctuations in the matrix except for the fact that it predicts zero stress fluctuations at the beginning of the plastic regime unlike the FE simulations. This has already been observed and commented in Section 5.1.1. But it is now observed in the case of combined isotropic and nonlinear hardening, that the agreement between the DIV formulation and the FE simulations is good, except for the full vanishing of the stress fluctuations at some stage on a new plastification after an elastic unloading. The loading stage at which this is observed coincides however very nicely with the minimum of the stress fluctuations in full-field simulations.

*5.2. Multiple cycles loadings*

We now investigate the predictions of the DIV formulation when the composite is submitted to $15$ radial loading cycles (program 2, Fig.1b). When applying such a loading to an elastically reinforced composite for which the elastoplastic matrix only exhibits nonlinear kinematic hardening without isotropic hardening, it is numerically observed that the macroscopic and local responses are stabilized as soon as the first cyclic loading occurs. This is not the case for an elastoplastic ma-

trix exhibiting combined isotropic and nonlinear kinematic hardening. For such a composite, we make use of the same material parameters as the ones used for the composite studied in the previous section except for the values of the nonlinear kinematic parameters which are now set as follows

$$a^{(2)} = 500\,\text{MPa} \quad \text{and} \quad \gamma^{(2)} = 40. \tag{98}$$

When applying multiple cycles loadings to the above-described elastically reinforced composites with combined isotropic and nonlinear kinematic hardening, we obtain the results depicted in Fig.5 Note that, for readability reasons, we only report in Fig.5c the 5 first cycles (red dotted line) and the $15^{\text{th}}$ cycle (black dotted line) of the FE simulations. First, it is observed a good agreement between the predictions of the DIV model and the numerical simulations for the effective stress and the average stress in the matrix. As observed on the macroscopic axial stress, the asymmetry characterising the Bauschinger effect decreases continuously with the number of cycles, going from $31.4\,\text{MPa}$ for the first cycle to $5.9\,\text{MPa}$ for the fifteenth cycle. This evolution of the asymmetry is accurately captured by the DIV formulation. It is also observed that, except for the first cycle, the predictions of the DIV model overestimates the FE simulations for the average stress in the inclusion. Similarly, the DIV formulation slightly overestimates the stress fluctuations in the matrix during the 7 first cycles (i.e. until $t = 150\,\text{s}$) and predicts zero fluctuations, unlike the FE simulations, at the beginning of the plastic reloadings. It is observed for the following cycles (from the $8^{\text{th}}$ to the $15^{\text{th}}$ cycle) that the FE simulations and the DIV predictions are very close and lead both to zero stress fluctuations at some identical stages in the loading cycle. This confirms the trend already discussed in previous sections for a single loading cycle. In addition, it is

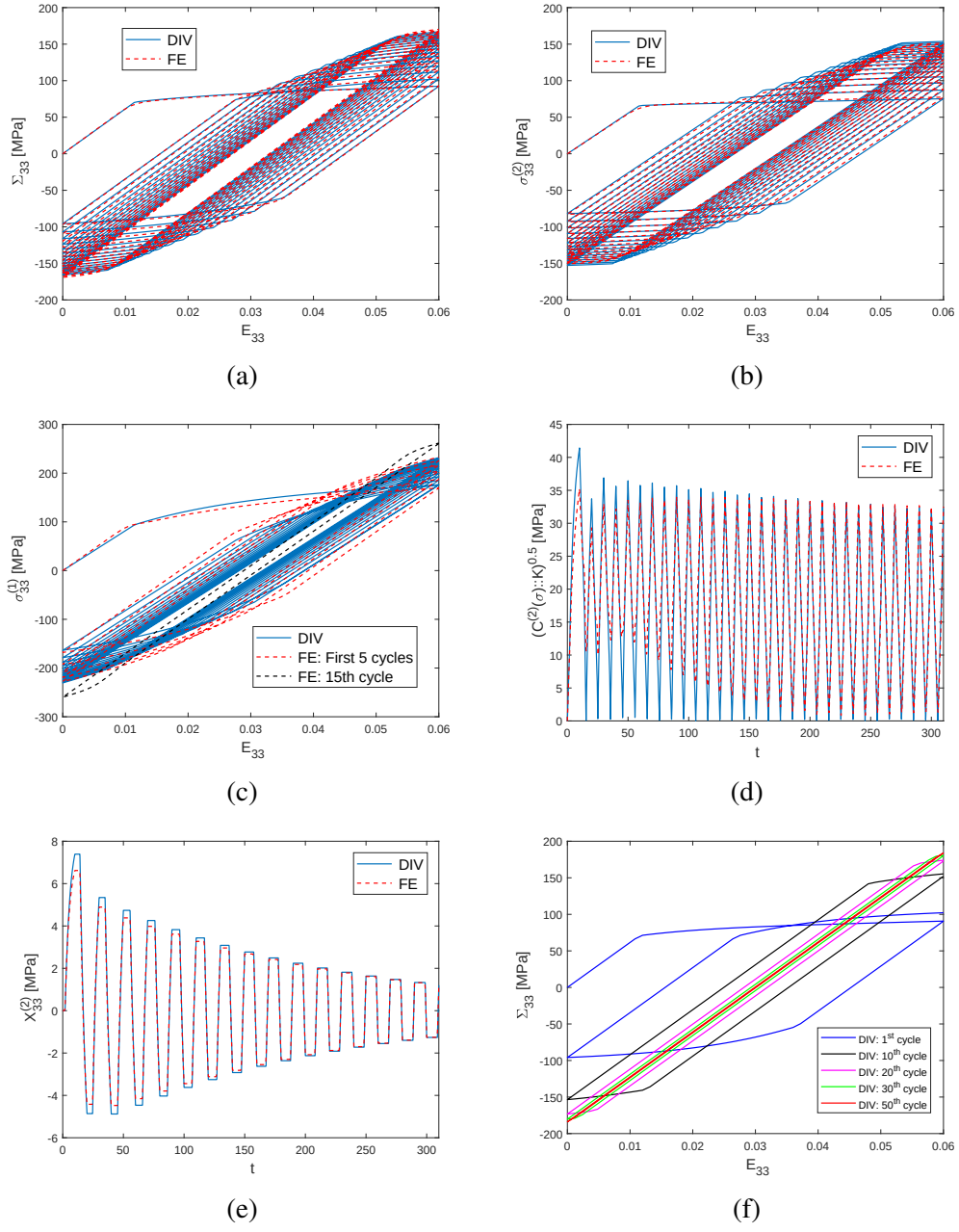


Figure 5: Elastically reinforced composite submitted to 15 loading cycles (program 2, Fig.1b). Case of an elastoplastic matrix with combined isotropic and nonlinear kinematic hardening. $c^{(1)} = 0.17$. Comparison between the DIV formulation and the FE simulations. (a) Macroscopic axial stress, (b) Average axial stress in the matrix, (c) Average axial stress in the inclusion, (d) Stress fluctuations in the matrix, (e) Matrix average of the axial back-stress, (f) DIV predictions of the macroscopic axial stress for 50 loading cycles.

now observed that the agreement between the DIV formulation and the FE simulations increases with the accumulation of cycles. Similarly a nice agreement, which in addition is even better for the last cycles, is observed for the evolution of the matrix average of the axial back-stress depicted in Fig.5e. Indeed, the DIV formulation only slightly overestimates the amplitude of the temporal evolution of this quantity w.r.t. the FE simulations for the $7$ first cycles and is nearly identical to the numerical results for the $8$ last ones.

In order to derive the asymptotic response of the composite, we submitted it to $50$ loading cycles. The results of the DIV simulations are depicted in Fig.5f. To analyse the asymptotic state, we did not compare the predictions of the DIV formulation to FE simulations. Indeed, as the DIV model reproduces very accurately the numerical simulations for 15 cycles loading (e.g. Fig.5a), we considered that the predictions of the DIV model are also accurate for 50 cycles. For reasons of readability, we only represent the first, $10^{\text{th}}$, $20^{\text{th}}$, $30^{\text{th}}$ and $50^{\text{th}}$ cycles. It is observed that the model predicts an elastic asymptotic response, i.e. an elastic shakedown.

## 6. Conclusion

In this study, we presented an extension of the DIV formulation proposed by Lucchetta et al. [1] to the context of composites made of elastoplastic phases with combined isotropic and nonlinear kinematic hardening. To this end, we considered the Armstrong-Frederick model which is based on the nonlinear kinematic hardening rule defined by Eq. (20). This model has been developed by Chaboche [5, 26] in the context of non-associated plasticity. In order to work in the framework of the incremental variational principles proposed by Lahellec and Suquet

[2], we made use of the modified Chaboche model [6] which is an approximation of the Armstrong-Frederick model and has the benefit to rely on the framework of materials whose behavior is governed by two potentials, as required by the use of the DIV formulation. Thanks to the work of Bouby et al. [27], we derived an expression of the dissipation potential $\varphi^{(r)}$ associated with the modified Chaboche model. It has been noted that the dissipation potential depends not only on the rate of the internal variables $\dot{\boldsymbol{\alpha}}$ but also on the internal state variables $\boldsymbol{\alpha}$. Because of this dependence, we have slightly modified in Section 2 the incremental variational principles introduced by Lahellec and Suquet [2]. Then, we introduced a linearized incremental potential $J_L$ and applied twice the variational procedure thus leading to a LCC with homogeneous polarization within the phases. The latter can be homogenized by classical linear mean-field homogenization schemes, here the Hashin-Shtrikman estimate. We also introduced some per-phase relaxations of the local constraints that apply on the internal variables in the variational optimization, which globally lead us to a system of nonlinear equations, with a limited number of unknowns. In order to close this system of nonlinear equations, we assumed that the fluctuations of the rate of the kinematic hardening variable $\dot{\boldsymbol{\nu}}$ are zero in phase $r$.

The DIV formulation has been applied to the case of composites made of two isotropic phases: an elastoplastic matrix with both isotropic and nonlinear kinematic hardening reinforced with linear elastic spherical particles. Then, it has been tested on two different composites submitted to a cyclic extension. The first one is made of an elastoplastic matrix with nonlinear kinematic hardening while in the second one the matrix exhibits both isotropic and nonlinear kinematic hardening. The predictions of the model have been compared to FE simulations that

we carried out. In both cases, an overall good agreement is observed for both the macroscopic response and the statistics of the local fields. Finally, we compared the predictions of the DIV formulation to FE simulations carried out for a loading of 50 cycles. It is observed that the DIV model accurately reproduces the numerical simulations at both the local and macroscopic scales and tends to an elastic asymptotic state corresponding to an elastic shakedown.

## AppendixA. Derivation of Eq. (42)

We start from Eq. (41) and notice by means of Eq. (39) that the dissipation potential $\varphi^{(r)}$ is present in the term $\Delta J$ of Eq. (41). Making use of the definition (31) of the dissipation potential $\varphi^{(r)}$, it is observed that $\Phi_{\mathcal{C}}(\dot{\boldsymbol{\varepsilon}}^p, \dot{p}) = +\infty$ when $g(\dot{\boldsymbol{\varepsilon}}^p, \dot{p}) > 0$ (see Eqs. (26) and (27)). Furthermore, as mentioned previously, only the first branch $\phi_1^{(r)}$ of the dissipation potential $\varphi^{(r)}$ (Eqs. (31) and (32)) is considered. The branch $\phi_1^{(r)}$ is associated with an inequality condition $h^{(r)}\left(\dot{\boldsymbol{\varepsilon}}^p, \dot{\boldsymbol{\nu}}\right) \leq 0$, where the function $h^{(r)}$ is defined, $\forall r \in [\![1, N]\!]$, by

$$h^{(r)}\left(\dot{\boldsymbol{\varepsilon}}^p, \dot{\boldsymbol{\nu}}\right) = \dot{\nu}_{eq} - \dot{\varepsilon}_{eq} \sqrt{\frac{4}{3}\frac{\gamma^{(r)}}{a^{(r)}}\left(\sigma_y^{(r)} + \frac{3}{4}\,a^{(r)}\gamma^{(r)}\left(\overline{\overline{\varepsilon_n^p + \nu_n}}^{(r)}\right)^2\right)}. \quad \text{(A.1)}$$

Accordingly, the infimum in Eq. (41) has to be sought for under the conditions $g\left(\frac{\boldsymbol{\varepsilon}^p - \boldsymbol{\varepsilon}_n^p}{\Delta t}, \frac{p - p_n}{\Delta t}\right) \leq 0$ and $h^{(r)}\left(\frac{\boldsymbol{\varepsilon}^p - \boldsymbol{\varepsilon}_n^p}{\Delta t}, \frac{\boldsymbol{\nu} - \boldsymbol{\nu}_n}{\Delta t}\right) \leq 0$ where $g$ and $h^{(r)}$ are defined by Eqs. (27) and (A.1), respectively. Note that at this stage these conditions need to be satisfied at all point $\underline{x} \in \Omega$. It is convenient to introduce the potential offset

$\Delta J_{bis}$ defined by

$$\Delta J_{bis}\left(\underline{x}, \boldsymbol{\varepsilon}^p, \boldsymbol{\nu}, p, \{\eta\}\right) = \sum_{r=1}^{N} \Delta J_{bis}^{(r)}\left(\underline{x}, \boldsymbol{\varepsilon}^p, \boldsymbol{\nu}, p, \eta^{(r)}\right)\, \chi^{(r)}(\underline{x}) \quad \text{with}$$

$$\begin{aligned}\Delta J_{bis}^{(r)}\left(\underline{x}, \boldsymbol{\varepsilon}^p, \boldsymbol{\nu}, p, \eta^{(r)}\right) =& \Delta t\, \phi_1^{(r)}\left(\left(\frac{\boldsymbol{\varepsilon}^p - \boldsymbol{\varepsilon}_n^p}{\Delta t}\right)_{eq}, \left(\frac{\boldsymbol{\nu} - \boldsymbol{\nu}_n}{\Delta t}\right)_{eq}\right) + \hat{w}^{(r)}\left(p_n + \frac{p - p_n}{\Delta t}\Delta t\right) \\ & - \frac{\eta_{\varepsilon^p}^{(r)}}{\Delta t}(\boldsymbol{\varepsilon}^p - \boldsymbol{\varepsilon}_n^p) : (\boldsymbol{\varepsilon}^p - \boldsymbol{\varepsilon}_n^p) - \frac{\eta_{\nu}^{(r)}}{\Delta t}(\boldsymbol{\nu} - \boldsymbol{\nu}_n) : (\boldsymbol{\nu} - \boldsymbol{\nu}_n),\end{aligned} \tag{A.2}$$

and

$$\phi_1^{(r)}\left(\dot{\varepsilon}_{eq}^p, \dot{\nu}_{eq}\right) = \left(\sigma_y^{(r)} + \frac{3}{4}\, a^{(r)}\gamma^{(r)}\left(\overline{\overline{\nu_n + \varepsilon_n^p}}\right)^2\right)\dot{\varepsilon}_{eq}^p + \frac{3}{4}\,\frac{a^{(r)}}{\gamma^{(r)}}\,\frac{\dot{\nu}_{eq}^2}{\dot{\varepsilon}_{eq}^p}, \tag{A.3}$$

such that

$$\tilde{w}_\Delta(\boldsymbol{E}) = \inf_{\langle\boldsymbol{\varepsilon}\rangle = \boldsymbol{E}} \left\{ \inf_{(\boldsymbol{\varepsilon}^p, \boldsymbol{\nu}, p)\,\Big/ \substack{h^{(r)}\left(\frac{\boldsymbol{\varepsilon}^p - \boldsymbol{\varepsilon}_n^p}{\Delta t}, \frac{\boldsymbol{\nu} - \boldsymbol{\nu}_n}{\Delta t}\right) \le 0 \\ g\left(\frac{\boldsymbol{\varepsilon}^p - \boldsymbol{\varepsilon}_n^p}{\Delta t}, \frac{p - p_n}{\Delta t}\right) \le 0}} \left\langle J_L(., \boldsymbol{\varepsilon}, \boldsymbol{\varepsilon}^p, \boldsymbol{\nu}, \{\eta\}) + \Delta J_{bis}(., \boldsymbol{\varepsilon}^p, \boldsymbol{\nu}, p, \{\eta\})\right\rangle \right\}. \tag{A.4}$$

Note that the term $\left(\overline{\overline{\nu_n + \varepsilon_n^p}}\right)^2$ in Eq. (A.3) results from the mean-field type approximation (40).

As in Lahellec and Suquet [2], an estimate of $\tilde{w}_\Delta$ can be derived by taking the supremum of $\Delta J_{bis}$ over ($\boldsymbol{\varepsilon}^p$, $\boldsymbol{\nu}$, $p$), separately over all positions $\underline{x} \in \Omega$, under the constraints $h^{(r)} \le 0$ and $g \le 0$. Furthermore, from (A.2), $\Delta J_{bis}$ can also be seen

as a function of ($\dot{\boldsymbol{\varepsilon}^p}$, $\dot{\boldsymbol{\nu}}$, $\dot{p}$). Accordingly, the potential $\tilde{w}_\Delta$ can be rewritten as

$$\begin{aligned}\tilde{w}_\Delta(\boldsymbol{E}) &\approx \tilde{w}_\Delta^{VAR}(\boldsymbol{E},\{\eta\}) \\ &= \inf_{\langle\boldsymbol{\varepsilon}\rangle=\boldsymbol{E}} \left\{ \begin{array}{l} \inf\limits_{(\boldsymbol{\varepsilon}^p,\boldsymbol{\nu},p)\Big/ \substack{h_1^{(r)}(\boldsymbol{\varepsilon}^p,\boldsymbol{\nu})\leq 0 \\ g_1(\boldsymbol{\varepsilon}^p,p)\leq 0}} \langle J_L(.,\boldsymbol{\varepsilon},\boldsymbol{\varepsilon}^p,\boldsymbol{\nu},\{\eta\})\rangle \\ \quad + \left\langle \sup\limits_{(\dot{\boldsymbol{\varepsilon}}^p,\dot{\boldsymbol{\nu}},\dot{p})\Big/ \substack{h^{(r)}(\dot{\boldsymbol{\varepsilon}}^p,\dot{\boldsymbol{\nu}})\leq 0 \\ g(\dot{\boldsymbol{\varepsilon}}^p,\dot{p})\leq 0}} \Delta J_{bis}(.,\dot{\boldsymbol{\varepsilon}}^p,\dot{\boldsymbol{\nu}},\dot{p},\{\eta\}) \right\rangle \end{array} \right\}, \end{aligned} \tag{A.5}$$

where $h_1^{(r)}$ and $g_1$ - which are simply a rewriting of $h^{(r)}$ and $g$ in a total formulation, i.e. depending on $\boldsymbol{\varepsilon}^p$, $\boldsymbol{\nu}$, $p$ instead of $\dot{\boldsymbol{\varepsilon}^p}$, $\dot{\boldsymbol{\nu}}$, $\dot{p}$ - read:

$$\begin{aligned} &h_1^{(r)}(\boldsymbol{\varepsilon}^p,\boldsymbol{\nu}) = (\boldsymbol{\nu}-\boldsymbol{\nu}_n):(\boldsymbol{\nu}-\boldsymbol{\nu}_n) - \\ &(\boldsymbol{\varepsilon}^p-\boldsymbol{\varepsilon}_n^p):(\boldsymbol{\varepsilon}^p-\boldsymbol{\varepsilon}_n^p)\left(\frac{4}{3}\frac{\gamma^{(r)}}{a^{(r)}}\left(\sigma_y^{(r)}+\frac{3}{4}a^{(r)}\gamma^{(r)}\left(\overline{\overline{\varepsilon_n^p+\nu_n}}^{(r)}\right)^2\right)\right) \\ &g_1(\boldsymbol{\varepsilon}^p,p) = (\boldsymbol{\varepsilon}^p-\boldsymbol{\varepsilon}_n^p):(\boldsymbol{\varepsilon}^p-\boldsymbol{\varepsilon}_n^p) - \frac{3}{2}(p-p_n)^2. \end{aligned} \tag{A.6}$$

Note that, due to approximation (40), $\tilde{w}_\Delta^{VAR}$ in Eq. (A.5) is only an estimate and not a rigorous upper bound of $\tilde{w}_\Delta$. However, as shown by Lahellec and Suquet [36, 2], such type of estimates can be too stiff in certain cases and can advantageously, be replaced by a sharper estimate through relaxing the supremum condition by a stationarity condition thus leading to Eq. (42).

## AppendixB. Expression of the second-order moments $\overline{\overline{\dot{\varepsilon}^p}}^{(r)}$ and $\overline{\dot{\nu}}^{(r)}$

Recalling that $\dot{\boldsymbol{\varepsilon}}^p = \frac{\boldsymbol{\varepsilon}^p - \boldsymbol{\varepsilon}^p_n}{\Delta t}$ and $\dot{\boldsymbol{\nu}} = \frac{\boldsymbol{\nu} - \boldsymbol{\nu}_n}{\Delta t}$, and making use of Eqs. (78) and (79), we obtain the following equations

$$\begin{aligned}(\Delta t)^2 \left(\overline{\overline{\dot{\varepsilon}^p}}^{(r)}\right)^2 = \left(A^{(r)}\right)^2 \left(\overline{\overline{\varepsilon_d}}^{(r)}\right)^2 + \left(B^{(r)} - 1\right)^2 \left(\overline{\overline{\varepsilon^p_n}}^{(r)}\right)^2 + \\ \left(C^{(r)}\right)^2 \left(\overline{\overline{\nu_n}}^{(r)}\right)^2 + \frac{4}{3} A^{(r)} \left(B^{(r)} - 1\right) \langle \boldsymbol{\varepsilon}_d : \boldsymbol{\varepsilon}^p_n \rangle^{(r)} + \\ \frac{4}{3} A^{(r)} C^{(r)} \langle \boldsymbol{\varepsilon}_d : \boldsymbol{\nu}_n \rangle^{(r)} + \frac{4}{3} C^{(r)} \left(B^{(r)} - 1\right) \langle \boldsymbol{\varepsilon}^p_n : \boldsymbol{\nu}_n \rangle^{(r)},\end{aligned} \tag{B.1}$$

and

$$\begin{aligned}(\Delta t)^2 \left(\overline{\dot{\nu}}^{(r)}\right)^2 = \left(P^{(r)}\right)^2 \left(\overline{\overline{\varepsilon_d}}^{(r)}\right)^2 + \left(Q^{(r)}\right)^2 \left(\overline{\overline{\varepsilon^p_n}}^{(r)}\right)^2 + \\ \left(R^{(r)} - 1\right)^2 \left(\overline{\overline{\nu_n}}^{(r)}\right)^2 + \frac{4}{3} P^{(r)} Q^{(r)} \langle \boldsymbol{\varepsilon}_d : \boldsymbol{\varepsilon}^p_n \rangle^{(r)} + \\ \frac{4}{3} P^{(r)} \left(R^{(r)} - 1\right) \langle \boldsymbol{\varepsilon}_d : \boldsymbol{\nu}_n \rangle^{(r)} + \frac{4}{3} Q^{(r)} \left(R^{(r)} - 1\right) \langle \boldsymbol{\varepsilon}^p_n : \boldsymbol{\nu}_n \rangle^{(r)}.\end{aligned} \tag{B.2}$$

In Eqs. (B.1) and (B.2), the quantities $\overline{\overline{\varepsilon^p_n}}^{(r)}$, $\overline{\overline{\nu_n}}^{(r)}$ and $\langle \boldsymbol{\varepsilon}^p_n : \boldsymbol{\nu}_n \rangle^{(r)}$ are known from the previous step and $\overline{\overline{\varepsilon_d}}^{(r)}$ is derived from the thermoelastic LCC $w_0$ (see Eqs. (72) and (B.5)). In order to fully determine $\overline{\overline{\dot{\varepsilon}^p}}^{(r)}$ and $\overline{\dot{\nu}}^{(r)}$, we need to compute $\langle \boldsymbol{\varepsilon}_d : \boldsymbol{\varepsilon}^p_n \rangle^{(r)}$ and $\langle \boldsymbol{\varepsilon}_d : \boldsymbol{\nu}_n \rangle^{(r)}$. First, we focus on the determination of $\langle \boldsymbol{\varepsilon}_d : \boldsymbol{\varepsilon}^p_n \rangle^{(r)}$. To this end, we start from

$$\begin{aligned}&\boldsymbol{\sigma}_d = \mathbb{K} : \frac{\partial\, w_L^{(r)}}{\partial\, \boldsymbol{\varepsilon}}(\boldsymbol{\varepsilon}) = 2\,\mu_L^{(r)}\,\boldsymbol{\varepsilon}_d + \boldsymbol{\tau}_L^{(r)} = 2\,\mu_L^{(r)}\,\boldsymbol{\varepsilon}_d - \delta_L^{(r)}\,\boldsymbol{\varepsilon}^p_n + \zeta_L^{(r)}\,\boldsymbol{\nu}_n, \\ &\text{with} \quad \delta_L^{(r)} = 2\,\mu^{(r)} B^{(r)} \quad \text{and} \quad \zeta_L^{(r)} = -2\mu^{(r)} C^{(r)},\end{aligned} \tag{B.3}$$

By multiplying Eq. (B.3) by it-self and averaging over phase $r$, we obtain

$$\langle \boldsymbol{\varepsilon}_d : \boldsymbol{\varepsilon}_n^p \rangle^{(r)} = \frac{1}{6\,\mu_L^{(r)}\,\delta_L^{(r)}} \left\{ \begin{array}{l} \left(3\,\mu_L^{(r)}\right)^2 \left(\overline{\overline{\varepsilon}_d}^{(r)}\right)^2 + \left(\frac{3}{2}\delta_L^{(r)}\right)^2 \left(\overline{\overline{\varepsilon_n^p}}^{(r)}\right)^2 + \left(\frac{3}{2}\zeta_L^{(r)}\right)^2 \left(\overline{\overline{\nu_n}}^{(r)}\right)^2 \\ + 6\mu_L^{(r)}\zeta_L^{(r)}\,\langle \boldsymbol{\varepsilon}_d : \boldsymbol{\nu}_n \rangle^{(r)} - 3\delta_L^{(r)}\zeta_L^{(r)}\,\langle \boldsymbol{\varepsilon}_n^p : \boldsymbol{\nu}_n \rangle^{(r)} - \left(\overline{\overline{\sigma_d}}^{(r)}\right)^2 \end{array} \right\}. \tag{B.4}$$

As mentioned in Section 4.3.1, the first and second-order moments $\overline{\boldsymbol{\varepsilon}_d}^{(r)}$, $\overline{\overline{\varepsilon}_d}^{(r)}$, $\overline{\overline{\sigma_d}}^{(r)}$ in expression (B.4) are approximated by $\overline{\boldsymbol{\varepsilon}_{0,d}}^{(r)}$, $\overline{\overline{\varepsilon}_{0,d}}^{(r)}$, $\overline{\overline{\sigma_{0,d}}}^{(r)}$, respectively. The first-order moment $\overline{\boldsymbol{\varepsilon}_{0,d}}^{(r)}$ is obtained by Eq. (82). Furthermore, $\overline{\overline{\varepsilon}_{0,d}}^{(r)}$ is given by

$$\overline{\overline{\varepsilon}_{0,d}}^{(r)} = \sqrt{\frac{2}{3}\langle \boldsymbol{\varepsilon}_{0,d} : \boldsymbol{\varepsilon}_{0,d} \rangle^{(r)}} = \sqrt{\frac{2}{3}\frac{1}{c^{(r)}}\frac{\partial\,\tilde{w}_0}{\partial\,\mu_0^{(r)}}(\boldsymbol{E})}, \tag{B.5}$$

while $\overline{\overline{\sigma_{0,d}}}^{(r)}$ is determined from

$$\boldsymbol{\sigma}_{0,d} = \frac{\partial\,w_0^{(r)}}{\partial\,\boldsymbol{\varepsilon}_{0,d}}(\boldsymbol{\varepsilon}_0) = 2\,\mu_0^{(r)}\,\boldsymbol{\varepsilon}_{0,d} + \boldsymbol{\tau}_0^{(r)}, \tag{B.6}$$

and reads

$$\overline{\overline{\sigma_{0,d}}}^{(r)} = \sqrt{\frac{3}{2}\left[6\left(\mu_0^{(r)}\right)^2\left(\overline{\overline{\varepsilon}_{0,d}}^{(r)}\right)^2 + \boldsymbol{\tau}_0^{(r)} : \boldsymbol{\tau}_0^{(r)} + 4\,\mu_0^{(r)}\boldsymbol{\tau}_0^{(r)} : \overline{\boldsymbol{\varepsilon}_{0,d}}^{(r)}\right]}. \tag{B.7}$$

We now get back to the evaluation of $\langle \boldsymbol{\varepsilon}_d : \boldsymbol{\nu}_n \rangle^{(r)}$ which is required to close the nonlinear system to be solved. For this, we make use of the following assumption: the fluctuations of $\dot{\boldsymbol{\nu}}$ are assumed to be zero in phase $r$, i.e.

$$C^{(r)}\left(\dot{\boldsymbol{\nu}}\right) :: \mathbb{K} = \mathbf{0} \Leftrightarrow \overline{\dot{\nu}}_{eq}^{(r)} = \overline{\overline{\dot{\nu}}}^{(r)}, \tag{B.8}$$

with $\overline{\dot{\nu}}_{eq}^{(r)} = \sqrt{\frac{2}{3}\,\overline{\dot{\boldsymbol{\nu}}}^{(r)} : \overline{\dot{\boldsymbol{\nu}}}^{(r)}}$.

Reporting (79), (B.2), (B.4) in (B.8) and isolating the term $\langle \boldsymbol{\varepsilon}_d : \boldsymbol{\nu}_n \rangle^{(r)}$, it comes

$$\langle \boldsymbol{\varepsilon}_d : \boldsymbol{\nu}_n \rangle^{(r)} = \frac{1}{\frac{4}{3}P^{(r)}\left(R^{(r)} - 1 + Q^{(r)}\,\frac{\zeta_L^{(r)}}{\delta_L^{(r)}}\right)} \times$$

$$\left\{ \begin{array}{l} \left(P^{(r)}\right)^2 \left( \left(\overline{\varepsilon_d}_{,eq}^{(r)}\right)^2 - \left(\overline{\overline{\varepsilon_d}}^{(r)}\right)^2 \right) + \left(Q^{(r)}\right)^2 \left( \left(\overline{\varepsilon_n^p}_{,eq}^{(r)}\right)^2 - \left(\overline{\overline{\varepsilon_n^p}}^{(r)}\right)^2 \right) \\ + \left(R^{(r)} - 1\right)^2 \left( \left(\overline{\nu_n}_{,eq}^{(r)}\right)^2 - \left(\overline{\overline{\nu_n}}^{(r)}\right)^2 \right) + \frac{4}{3}Q^{(r)} \left(R^{(r)} - 1\right) \left( \overline{\boldsymbol{\varepsilon}_n^p}^{(r)} : \overline{\boldsymbol{\nu}_n}^{(r)} - \langle \boldsymbol{\varepsilon}_n^p : \boldsymbol{\nu}_n \rangle^{(r)} \right) \\ + \frac{4}{3}P^{(r)} \left(R^{(r)} - 1\right) \overline{\boldsymbol{\varepsilon}_d}^{(r)} : \overline{\boldsymbol{\nu}_n}^{(r)} + \frac{4}{3}P^{(r)}Q^{(r)}\, \overline{\boldsymbol{\varepsilon}_d}^{(r)} : \overline{\boldsymbol{\varepsilon}_n^p}^{(r)} \\ - \frac{2}{9}\frac{P^{(r)}Q^{(r)}}{\mu_L^{(r)}\,\delta_L^{(r)}} \left[ \begin{array}{l} \left(3\,\mu_L^{(r)}\right)^2 \left(\overline{\overline{\varepsilon_d}}^{(r)}\right)^2 + \left(\frac{3}{2}\delta_L^{(r)}\right)^2 \left(\overline{\overline{\varepsilon_n^p}}^{(r)}\right)^2 + \left(\frac{3}{2}\zeta_L^{(r)}\right)^2 \left(\overline{\overline{\nu_n}}^{(r)}\right)^2 \\ - 3\delta_L^{(r)}\zeta_L^{(r)} \langle \boldsymbol{\varepsilon}_n^p : \boldsymbol{\nu}_n \rangle^{(r)} - \left(\overline{\overline{\sigma_d}}^{(r)}\right)^2 \end{array} \right] \end{array} \right\}, \tag{B.9}$$

where the second-order moments $\overline{\overline{\varepsilon_d}}^{(r)}$ and $\overline{\overline{\sigma_d}}^{(r)}$ are still approximated by $\overline{\overline{\varepsilon_{0,d}}}^{(r)}$ and $\overline{\overline{\sigma_{0,d}}}^{(r)}$ which are evaluated by Eqs. (B.5) and (B.7). Note that all the other terms of expression (B.9) are known from the former time step.

## References


[1] A. Lucchetta, F. Auslender, M. Bornert, D. Kondo, A double incremental variational procedure for elastoplastic composites with combined isotropic and linear kinematic hardening, International Journal of Solids and Structures 158 (2019) 243–267.

[2] N. Lahellec, P. Suquet, On the effective behavior of nonlinear inelastic composites: I. Incremental variational principles, Journal of the Mechanics and Physics of Solids 55 (2007) 1932–1963.

[3] M. Agoras, R. Avazmohammadi, P. Ponte Castañeda, Incremental vari-

ational procedure for elasto-viscoplastic composites and application to polymer- and metal-matrix composites reinforced by spheroidal elastic particles, International Journal of Solids and Structures 97-98 (2016) 668–686.

[4] P. J. Armstrong, C. O. Frederick, A mathematical representation of the multiaxial bauschinger effect, CEGB Report RD/B/N731.

[5] J.-L. Chaboche, Sur l'utilisation des variables d'état interne pour la description de la viscoplasticité cyclique avec endommagement, in: Problème Non Linéaire de Mécanique, Symposium Franco-Polonais de Rhéologie et Mécanique, Cracovie, 1977.

[6] J.-L. Chaboche, Constitutive equations in creep-fracture damage, in: Wilshire, Owen (Eds.), Engineering Approaches to High Temperature Design, Pineridge-Press, Swansea, 1983.

[7] P. Ponte Castañeda, The effective mechanical properties of nonlinear isotropic composites, Journal of the Mechanics and Physics of Solids 39 (1991) 45–71.

[8] B. Halphen, Q. Nguyen, Sur les matériaux standard généralisés, Journal de Mécanique 14 (1975) 39–63.

[9] J. Lemaître, J. Chaboche, Mechanics des matériaux solides, Dunod, Paris, 1985.

[10] Q. S. Nguyen, Mechanical modelling of anelasticity, Revue de Physique Appliquée 1988 (1988) 325–330.

[11] P. Germain, Q. S. Nguyen, P. Suquet, Continuum thermodynamics, Journal of Applied Mechanics 50 (1983) 1010–1020.

[12] M. Ortiz, L. Stainier, The variational formulation of viscoplastic constitutive updates, Computer Methods in Applied Mechanics and Engineering 171 (1999) 419–444.

[13] L. Brassart, L. Stainier, I. Doghri, L. Delannay, Homogenization of elasto-(visco) plastic composites based on an incremental variational principle, International Journal of Plasticity 36 (2012) 86–112.

[14] N. Lahellec, P. Suquet, Effective response and field statistics in elast-plastic and elasto-viscoplastic composites under radial and non radial loading, International Journal of Plasticity 42 (2013) 1–30.

[15] J. Boudet, F. Auslender, M. Bornert, Y. Lapusta, An incremental variational formulation for the prediction of the effective work-hardening behavior and field statistics of elasto-(visco)plastic composites, International Journal of Solids and Structures 83 (2016) 90–133.

[16] M. Idiart, N. Lahellec, Estimates for the overall linear properties of pointwise heterogeneous solids with application to elasto-viscoplasticity, Journal of the Mechanics and Physics of Solids 97 (2016) 317–332.

[17] S. Mercier, K. Kowalczyk-Gajewska, C. Czarnota, Effective behavior of composites with combined kinematic and isotropic hardening based on additive tangent mori–tanaka scheme, Composites Part B 174 (2019) 1–30.

[18] A. Molinari, G. R. Canova, S. Ahzi, A self consistent approach of the large

deformation polycrystal viscoplasticity, Acta Metallurgica 35 (1987) 2983–2994.

[19] S. Mercier, A. Molinari, Validation of an interaction law for the eshelby inclusion problem in elasto-viscoplasticity, International Journal of Solids and Structures 42 (2009) 1923–1941.

[20] I. Doghri, A. Ouaar, Homogenization of two-phase elasto-plastic composite materials and structures. study of tangent operators, cyclic plasticity and numerical algorithms, International Journal of Solids and Structures 40 (2003) 1681–1712.

[21] R. Hill, Continuum micro-mechanics of elastoplastic polycrystals, Journal of the Mechanics and Physics of Solids 13 (1965) 89–101.

[22] J. C. Michel, P. Suquet, A model-reduction approach in micromechanics of materials preserving the variational structure of constitutive relations, Journal of the Mechanics and Physics of Solids 90 (2016) 254–285.

[23] Q. S. Nguyen, Stability and Nonlinear Solid Mechanics, John Wiley and Sons Ltd, Chichester, 2000.

[24] L. Brassart, L. Stainier, On convergence properties of variational constitutive updates for elasto-visco-plasticity, GAMM-Mitt 35 (2012) 26–42.

[25] P. J. Armstrong, C. O. Frederick, A mathematical representation of the multiaxial bauschinger effect, Materials at High Temperatures 24 (2007) 1–26.

[26] J.-L. Chaboche, Description phénoménologique de la viscoplasticité cy-

clique avec endommagement, Ph.D. thesis, Université Pierre et Marie Curie, Paris 6 (1978).

[27] C. Bouby, D. Kondo, G. de Saxcé, A comparative analysis of two formulations for non linear hardening plasticity models: Application to shakedown analysis, European Journal of Mechanics - A/Solids 53 (2015) 48–61.

[28] A. Lucchetta, Homogénéisation des composites élasto-viscoplastiques écrouissables par une double procédure variationnelle incrémentale, Ph.D. thesis, Sorbonne University (2019).

[29] N. Lahellec, P. Ponte Castañeda, P. Suquet, Variational estimates for the effective response and field statistics in thermoelastic composites with intraphase property fluctuations, Proceeding of the Royal Society A 447 (2011) 2224–2246.

[30] P. Ponte Castañeda, New variational principles in plasticity and their application to composite materials, Journal of the Mechanics and Physics of Solids 40 (1992) 1757–1788.

[31] J. Cotelo, S. Das, P. Ponte Castañeda, A differential homogenization method for estimating the macroscopic response and field statistics of particulate viscoelastic composites, International Journal of Solids and Structures 204-205 (2020) 199–219.

[32] M. Idiart, N. Lahellec, P. Suquet, Model reduction by mean-field homogenization in viscoelastic composites: I. Primal theory, Proceedings of the Royal Society A 416 (2020) 1–16.

[33] M. Idiart, N. Lahellec, P. Suquet, Model reduction by mean-field homogenization in viscoelastic composites: II. Application to rigidly reinforced solids, Proceedings of the Royal Society A 416 (2020) 17–38.

[34] A. Rekik, F. Auslender, M. Bornert, A. Zaoui, Objective evaluation of linearization procedures in nonlinear homogenization: A methodology and some implicationson the accuracy of micromechanical schemes, International Journal of Solids and Structures 44 (2007) 3468—-3496.

[35] M. Majewski, P. Holobut, M. Kursa, K. Kowalczyk-Gajewska, Packing and size effects in elastic-plastic particulate composites: Micromechanical modelling and numerical verification, International Journal of Engineering Science 151 (2020) 1–18.

[36] N. Lahellec, P. Suquet, Effective behavior of linear viscoelastic composites: a time-integration approach, International Journal of Solids and Structures 44 (2006) 507–529.